

SUSX-TH/96-003, OUTP-96-01P, IEM-FT-125/96

hep-ph/9602381

R-parity Violation Effects through Soft Supersymmetry Breaking Terms and the Renormalisation Group

B. de Carlos¹ and P. L. White²¹*School of Mathematical and Physical Sciences, University of Sussex,**Falmer, Brighton BN1 9QH, UK.**Email: B.De-Carlos@sussex.ac.uk**and*²*Theoretical Physics, University of Oxford,**1 Keble Road, Oxford OX1 3NP, UK.**Email: plw@thphys.ox.ac.uk*

Abstract

We present full renormalisation group equations for the MSSM with R-parity violation, including all soft supersymmetry breaking terms. The inclusion of dimensionless R-parity violating couplings can generate many possible low energy effects through the generation of off-diagonal soft masses violating lepton and quark flavour, and through the generation of lepton-Higgs mixing. We discuss the relation between the weak and unification scale R-parity violation and study the effects on neutrino mass generation and $\mu \rightarrow e\gamma$.

1 Introduction

Among the different proposals to extend the Standard Model (SM), supersymmetric models are probably the most attractive ones as their fundamental ingredient, supersymmetry (SUSY) [1], provides a very elegant solution to the so-called hierarchy problem. However the most popular SUSY extension of the SM is not the most general one, as it is commonly assumed that a discrete symmetry, known as R-parity, forbids all the baryon (B) and lepton (L) number violating couplings, hence avoiding possible rapid proton decay. To each field is assigned an R-parity given by $R \equiv (-1)^{3B+L+2S}$ (S being the spin) so that all the SM particles have $R = +1$ while their SUSY partners have $R = -1$. Immediate consequences of imposing such a symmetry are that SUSY particles are produced in pairs and that the lightest SUSY particle (LSP) is stable, therefore becoming a dark matter candidate.

However, there is no obvious reason why B or L violating interactions should not be allowed separately to break R-parity [2, 3], and the apparent constraints through the requirement that any new physics should not ruin baryogenesis in the early universe have been shown to be very weak [4]. The corresponding terms in the superpotential are:

$$W_B = \frac{1}{2} \lambda''_{ijk} u_i d_j d_k \quad (1.1)$$

and

$$W_L = \frac{1}{2} \lambda_{ijk} L_i L_j e_k + \lambda'_{ijk} L_i Q_j d_k \quad , \quad (1.2)$$

where u , d , e stand for the u-type, d-type and lepton singlet superfields, and Q , L are the quark and lepton doublet superfields respectively, which generate dimensionless couplings in the Lagrangian, given by:

$$\mathcal{L}_B = \frac{1}{2} \lambda''_{ijk} (u_i^c d_j^c \tilde{d}_k^* + u_i^c \tilde{d}_j^* d_k^c + \tilde{u}_i^* d_j^c d_k^c) + \text{h.c.} \quad (1.3)$$

and:

$$\begin{aligned}
\mathcal{L}_{\cancel{B}} = & \frac{1}{2}\lambda_{ijk} \left(\bar{\nu}_{Li}^c e_{Lj} \tilde{e}_{Rk}^* - e_{Li} \bar{\nu}_{Lj}^c \tilde{e}_{Rk}^* + \nu_{Li} \tilde{e}_{Lj} \bar{e}_{Rk} - e_{Li} \tilde{\nu}_{Lj} \bar{e}_{Rk} \right. \\
& \left. + \tilde{\nu}_{Li} e_{Lj} \bar{e}_{Rk} - \tilde{e}_{Li} \nu_{Lj} \bar{e}_{Rk} \right) + \text{h.c.} \\
& + \lambda'_{ijk} \left(\bar{\nu}_{Li}^c d_{Lj} \tilde{d}_{Rk}^* - \bar{e}_{Ri} u_{Lj} \tilde{d}_{Rk}^* + \nu_{Li} \tilde{d}_{Lj} \bar{d}_{Rk} - e_{Li} \tilde{\nu}_{Lj} \bar{d}_{Rk} \right. \\
& \left. + \tilde{\nu}_{Li} d_{Lj} \bar{d}_{Rk} - \tilde{e}_{Li} u_{Lj} \bar{d}_{Rk} \right) + \text{h.c.}
\end{aligned} \tag{1.4}$$

Besides these, we also expect dimensionful terms analogous to the R-parity conserving *soft breaking terms*; that is, we get soft trilinear couplings and masses which violate B or L :

$$V_{\cancel{B} \text{ soft}} = \frac{1}{2} C''_{ijk} \tilde{u}_i \tilde{d}_j \tilde{d}_k + \text{h.c.} + \sum_{a,b} m_{ab}^2 \varphi_a \bar{\varphi}_b \tag{1.5}$$

$$V_{\cancel{L} \text{ soft}} = \frac{1}{2} C_{ijk} \tilde{L}_i \tilde{L}_j \tilde{e}_k + C'_{ijk} \tilde{L}_i \tilde{Q}_j \tilde{d}_k + \text{h.c.} + \sum_{a,b} m_{ab}^2 \varphi_a \bar{\varphi}_b + D_i \tilde{L}_i H_2 + \text{h.c.} \tag{1.6}$$

Here the soft masses shown include such terms as $m_{L_i H_1}^2$ which violates L , and also terms violating lepton and quark flavour symmetries (where each generation is assigned its own L_i and B_i) whose effects will be in addition to the contribution from the CKM sector. For a discussion of our notation, see Appendix A.

R-parity violation has been considered by many authors in the past and recently there has been an increasing interest in the renormalisation group properties of R-parity violating couplings [5, 6, 7, 8]. This is specially interesting when we try to embed the SM as the low energy limit of a more fundamental Grand Unified Theory (GUT). In such a framework we have a prediction for the values of the different couplings at the unification scale, M_{GUT} , and we can therefore use their renormalisation group equations (RGEs) to obtain the corresponding values at low energies and compare them with the existing limits. This applies to both dimensionless and dimensionful couplings, for which the RGEs are given (the latter for the first time) in Appendix A.

Concerning the limits which can be imposed on these couplings, there have been many attempts to constrain them through their impact on rare processes in the laboratory [9, 10, 11] and it turns out that flavour changing neutral current (FCNC) processes in particular provide us with a very powerful tool to test physics beyond the SM. The presence of extra particles, SUSY partners in this case, together with lepton and quark flavour violating couplings, including here off-diagonal soft masses, in our fundamental theory can induce transitions forbidden in the pure SM and, moreover, strongly constrained by experiment. Consequently an upper bound can be derived on different products of dimensionless couplings and even on some of the dimensionful ones. Furthermore, some of these newly generated couplings can give rise to neutrino masses and mixings which are again experimentally constrained.

In general we expect that once we allow the violation of lepton and quark flavour symmetries through any operator, including the R-parity violating dimensionless couplings shown in equations (1.2) and (1.3), other such operators will be generated through the RGEs. In particular, we here study for the first time how the R-parity violating couplings generate soft terms which can lead to large FCNC effects in the lepton sector process $\mu \rightarrow e\gamma$.

Therefore, the aim of this paper is to present a detailed study of the limits which can be obtained on these R-parity violating couplings *at the GUT scale* by imposing FCNC and neutrino mass bounds *at low energy*. In particular, we have focussed on L violating interactions, but we plan to study B violation in a forthcoming paper.

In section 2 we discuss the dimensionless R-parity violating couplings. We sketch analytical solutions for the case when the gauge contribution dominate in their RGEs and obtain triviality bounds for different values of the strong coupling α_3 . In section 3 we clarify which basis is the most appropriate to deal with lepton and quark flavour violation and also the lepton-Higgs (LH) mixing which arises from R-parity

violation. Section 4 is devoted to a study of sneutrino VEVs, their generation from the dimensionful RGEs, and the limits which can be set on them by using the present constraints on neutrino masses. In section 5 we put limits on various R-parity violating couplings at M_{GUT} by running them to the electroweak scale and requiring that the full SUSY contribution to the FCNC process $\mu \rightarrow e\gamma$ be less than its actual experimental bound. We perform a full numerical study and give some analytical approximations. Finally in section 6 we present our conclusions.

2 Dimensionless Couplings

Before turning to the dimensionful couplings, it will be helpful to discuss what conclusions we can draw from the RGEs in Appendix A with respect to the dimensionless ones. We start by remarking that there have recently been a number of analyses [5, 6, 7, 8] studying the RGEs for some or all of the dimensionless couplings. Our RGEs are consistent with both references [5] and [6], apart from a couple of typographical errors in the gauge contributions to the RGEs in reference [5]. More complete lists of RGEs are given in reference [7], but here we disagree on a number of coefficients, even at one loop. Our equations give a different sign for the third term in equation (2.13) and the last term in (2.16) of that paper. Finally, we agree with the equations of reference [8].

While the equations are too complex to be usefully solved analytically in general, we might expect that often many (or all) of the R-parity violating Yukawa couplings will be tiny relative to the gauge couplings, and hence that only the effect of the latter will be relevant. In this limit, it is straightforward to solve the RGEs analytically [12] as follows.

$$\begin{aligned}\tilde{\alpha}_a(t) &= \frac{\tilde{\alpha}_a(t_0)}{1 - 2b_a(t - t_0)\tilde{\alpha}_a(t_0)} \\ \lambda(t) &= \left(1 - 22(t - t_0)\tilde{\alpha}_1(t_0)\right)^{c_1/22} \left(1 - 2(t - t_0)\tilde{\alpha}_2(t_0)\right)^{c_2/2}\end{aligned}$$

$$\begin{aligned}
& \times \left(1 + 6(t - t_0)\tilde{\alpha}_3(t_0)\right)^{-c_3/6} \\
\lambda'(t) &= \left(1 - 22(t - t_0)\tilde{\alpha}_1(t_0)\right)^{c'_1/22} \left(1 - 2(t - t_0)\tilde{\alpha}_2(t_0)\right)^{c'_2/2} \\
& \times \left(1 + 6(t - t_0)\tilde{\alpha}_3(t_0)\right)^{-c'_3/6} \\
\lambda''(t) &= \left(1 - 22(t - t_0)\tilde{\alpha}_1(t_0)\right)^{c''_1/22} \left(1 - 2(t - t_0)\tilde{\alpha}_2(t_0)\right)^{c''_2/2} \\
& \times \left(1 + 6(t - t_0)\tilde{\alpha}_3(t_0)\right)^{-c''_3/6}
\end{aligned} \tag{2.1}$$

Here we have used the convention that $t = \ln \mu$ where μ is the \overline{MS} renormalisation scale, while

$$\begin{aligned}
\tilde{\alpha}_a &= g_a^2/(16\pi^2) \\
b_a &= (11, 1, -3) \\
c_a &= (3, 3, 0) \\
c'_a &= (7/9, 3, 16/3) \\
c''_a &= (4/3, 0, 8)
\end{aligned} \tag{2.2}$$

and the label a runs over gauge groups 1,2,3. Although it is possible to derive analytical solutions even when the Yukawa couplings are large [12], in practice the expressions become so complicated that they are not particularly useful.

If we solve these equations with $t = \ln(M_{GUT}/M_Z)$, and using $M_{GUT} = 2 \times 10^{16}\text{GeV}$, $\alpha_3 = 0.11, 0.12, 0.13$, we find

$$\begin{aligned}
\lambda(M_Z) &= 1.5 \lambda(M_{GUT}) \\
\lambda'(M_Z) &= 3.4, 3.6, 3.7 \lambda'(M_{GUT}) \\
\lambda''(M_Z) &= 4.0, 4.3, 4.7 \lambda''(M_{GUT})
\end{aligned} \tag{2.3}$$

These results break down at the 10% level only when $\lambda(M_Z)$, $\lambda'(M_Z)$, $\lambda''(M_Z)$ exceed 0.27, 0.15, 0.15, which are very much larger than the values which we shall consider in our FCNC and neutrino calculations. For the R-parity violating couplings which

couple directly to h_t (and, for sufficiently large $\tan \beta$, to h_b) the ratio of the low energy to high energy value is reduced somewhat, typically by up to around 20%.

Another interesting feature, and one which has been discussed in a number of recent papers [5, 6, 7, 8], is that it is possible to derive triviality bounds on the R-parity violating couplings in exactly the same way as for the top quark Yukawa. Such bounds depend quite strongly on the values of $\tan \beta$ and α_3 . We give bounds derived from our RGEs in Table 1 by simply setting the coupling to be very large at the GUT scale, either with small h_t or h_t also at triviality, and running down to a scale of order the top mass. These results agree quite well with those of references [5, 6], and agree also with those given in reference [8] where applicable.

Coupling	Limit, $\alpha_3 = 0.11$	Limit, $\alpha_3 = 0.12$	Limit, $\alpha_3 = 0.13$
λ	0.92	0.92	0.92
λ'	1.08	1.10	1.12
λ''	1.17	1.20	1.23
λ	0.92 (1.08)	0.92 (1.11)	0.92 (1.13)
λ'_{xxx}	1.08 (1.08)	1.10 (1.11)	1.12 (1.13)
λ'_{x3x}	1.00 (1.00)	1.02 (1.03)	1.04 (1.04)
λ''_{xxx}	1.17 (1.08)	1.20 (1.11)	1.23 (1.13)
λ''_{3xx}	1.02 (0.93)	1.05 (0.95)	1.08 (0.96)

Table 1. Triviality limits on various couplings derived firstly by considering h_t small, and secondly in the case where h_t approaches its triviality limit. In the latter case we show the low energy value of h_t in brackets. Here “x” can represent either 1 or 2 (or 3 if the index corresponds to an L or e and we are not in the very large $\tan \beta$ regime), and the calculation has been performed for a variety of different $\alpha_3(M_Z)$.

3 Choice of Basis

We shall be interested in deriving constraints on R-parity violation which arise through lepton flavour violation (LFV), in which processes are allowed to violate lepton number generation by generation, quark flavour violation (QFV), or the mixing between leptonic and higgs superfields (LH mixing). Given the nature of these effects, it will be convenient here to discuss our choice of basis, and how this basis

affects our calculations. Indeed, it has recently been pointed out that bounds derived in a quark mass eigenstate basis can be rather different from those derived with the same couplings in a weak eigenstate basis [13]. While the physics is invariant, it is important that we choose a convenient (and consistent) basis to work in.

It is well known that, by judicious rotations of the fermion fields in the Standard Model, it is possible to work in a basis where the mass eigenstates are as far as possible weak eigenstates, thus eliminating FCNC at tree level and ensuring lepton flavour conservation at all orders even through charged current processes. In terms of supersymmetric parameters, the three fermion mass matrices correspond to Yukawa matrices h_{ij}^e , h_{ij}^u , h_{ij}^d of which the first two can be simultaneously diagonalised. Given the usual assumptions of universality at the GUT scale, the soft mass matrices are diagonal while the trilinear terms are proportional to the corresponding Yukawas, and so there is no LFV, and the only QFV effects beyond the usual SM ones are those coming from the CKM matrix, which are relatively small [14, 15]. This picture can break down when non-universal soft masses are allowed at the GUT scale, for example because one is considering a realistic unified theory, but this is outside the scope of our analysis.

It is clear from the RGEs presented in Appendix A that for some arbitrary choice of R-parity violating couplings there will be LFV, QFV, and LH mixing effects. The last case, for example, is driven through diagrams of the type shown in Figure 1. These generate non-diagonal anomalous dimension matrix elements of form $\gamma_{Li}^{H_1}$ which violate lepton number, and analagous diagrams exist which conserve L and B but generate LFV or QFV. With the insertion of appropriate spurion terms for the soft masses we will also find LFV and QFV effects in the soft sector.

Thus, even working in a basis where the Yukawa matrices which generate the fermion masses are diagonal at the GUT scale, this will not necessarily be true at the

electroweak scale. It is simplest then to invoke the GIM mechanism and to perform a field rotation so as to eliminate the most awkward effects and simplify calculations, which we find to be the quark and lepton mass eigenstate basis. The question now is what effect this rotation will have on the LFV, QFV and LH mixing terms in the soft sector.

Continuing with the case of LFV, in general this field rotation must take the form $L \rightarrow UL$, $e \rightarrow V^*e$, suppressing all indices for simplicity, so that

$$Lh^e e H_1 \rightarrow L(U^T h^e V^*) e H_1 \quad (3.1)$$

with U and V unitary matrices selected so that $(U^T h^e V^*)$ is diagonal. We now consider the effect of this rotation on the slepton mass matrices. We find that

$$m_L^2 \rightarrow \tilde{m}_L^2 := U^\dagger m_L^2 U \quad (3.2)$$

If we assume that

$$m_L^2 = m^2 \times I + \delta m^2 \quad (3.3)$$

where I is the identity matrix and δm^2 is a matrix with the only non-zero elements small and off-diagonal, while similarly $U = I + O(\varepsilon)$ with ε parametrising the rotation and assumed to be small, we can see that

$$\tilde{m}_L^2 = m_L^2 + O(\varepsilon \delta m^2) \quad (3.4)$$

Clearly, if we have sufficiently small off-diagonal elements in the mass and Yukawa matrices, we are quite safe in taking the non-diagonal terms in the mass-matrix to be the same before and after we have rotated back into the appropriate mass eigenstate basis. It is straightforward to check that this argument is valid for all the LFV effects which we consider.

The argument above assumes degenerate masses for the relevant generations and so will clearly be inaccurate in the case of any process involving the third generation,

such as $b \rightarrow s\gamma$, and for the case where we consider LH mixing. Here there is no alternative but to perform the rotation into the appropriate basis explicitly. The case for LH mixing is somewhat different, since here the preferred basis for simplicity is not a mass eigenstate basis but one in which there are no couplings in the superpotential of form $\mu_i L_i H_2$, but the same principle applies. As will be shown explicitly in the next section, even continuously rotating the fields so as to ensure that μ_i remains zero at all scales will not remove all the LH mixing effects in, for example, the running of the Yukawa couplings, the soft bilinear terms, and $m_{L_i H_1}^2$.

We conclude by noting that in the fermion mass eigenstate basis the non-diagonal soft masses will appear in the form of flavour violating mass insertions in our diagrams, rather than in the vertices themselves.

4 Sneutrino VEVs

4.1 General Discussion

One signature of R-parity violation which has been much discussed is that of sneutrino VEVs. These typically arise because of the existence of μ_i , D_i , and $m_{L_i H_1}^2$ terms which explicitly cause the effective potential to contain terms linear in the sneutrino field, either from explicit [3, 16] or spontaneous [17] R-parity violation (the origin of R-parity violation is irrelevant if it appears in this sector, and recently the implications of such effects have been considered in the context of GUTs [18]). They can also be caused by one loop effects involving dimensionless R-parity violating couplings [19, 20].

Once sneutrinos have acquired VEVs, neutrinos and neutralinos mix¹, so that we may derive bounds on R-parity violating terms by imposing experimental limits on neutrino masses. In fact, it has recently been shown that it is possible not merely

¹As in fact, charginos and leptons, and Higgses and sneutrinos

to bound R-parity violating terms, but to select such terms so as to explain the present rather complicated array of experimental measurements of neutrino masses and oscillations [21].

The potential which we must minimise takes the form

$$\begin{aligned}
V = & (m_{H_1 H_1}^2 + \mu_4^2)\nu_1^2 + (m_{H_2 H_2}^2 + \mu_4^2)\nu_2^2 + 2D_4\nu_1\nu_2 + \frac{g_1^2 + g_2^2}{8}(\nu_1^2 - \nu_2^2)^2 \\
& + 2(m_{H_1 L_i}^2 + \mu_4\mu_i)\nu_1 l_i + 2D_i l_i \nu_2 \\
& + (m_{L_i L_j}^2 + \mu_i\mu_j)l_i l_j + \frac{g_1^2 + g_2^2}{4}l_i^2(\nu_1^2 - \nu_2^2)
\end{aligned} \tag{4.1}$$

Here l_i is the VEV of L_i , with i, j running from 1 to 3, we drop all terms of order l^3 and above (since we expect $l \ll \nu$). We define as usual $\nu_i = \langle H_i \rangle$, with $\nu^2 = \nu_1^2 + \nu_2^2 = (174\text{GeV})^2$ and $\tan \beta = \nu_2/\nu_1$.

In order to study these effects, it is most convenient to follow reference [3], and perform a field rotation mixing the L_i and H_1 such that only one of the μ_i , which we choose to be μ_4 , is non-zero. Doing so will not merely change the dimensionful couplings, but will also generate new contributions to the dimensionless couplings λ and λ' from h_τ and h_t . In this basis, however, both the Higgs-sneutrino potential and the neutrino-neutralino mass matrix take on relatively simple forms. Up to order l/ν , and assuming that the off-diagonal terms in the mass matrix $m_{L_i L_j}^2$ are small, we find that

$$l_i = -\frac{D_i\nu_2 + m_{H_1 L_i}^2\nu_1}{m_{L_i}^2 + \frac{1}{2}M_Z^2 \cos 2\beta} \tag{4.2}$$

There are two dangerous approximations which we have made and which should be justified. The first is that we have only considered the Higgs potential at tree level. This is well known not to be reliable in general, but we would not expect that the large radiative corrections due to quark and squark loops should greatly affect the calculation of sneutrino VEVs. Hence we expect our analysis to be reliable so long as we derive the Higgs VEVs ν_1, ν_2 from the full one-loop effective potential before substituting them into equation (4.2).

Our second approximation is that we have not considered the processes discussed in detail in reference [20], in which one-loop diagrams generate sneutrino VEVs even with all dimensionful R-parity violating couplings zero. We shall ignore this point, and simply draw the reader's attention to the fact that the effects we study will in general be supplementary to these.

The neutralino-neutrino mass matrix then takes the form, in the basis of 2-spinors given by $\{i\tilde{B}^0, i\tilde{W}_3^0, \tilde{H}_1^0, \tilde{H}_2^0, L_i\}$,

$$\begin{pmatrix} M_1 & 0 & -\frac{1}{\sqrt{2}}g_1\nu_1 & \frac{1}{\sqrt{2}}g_1\nu_2 & -\frac{1}{\sqrt{2}}g_1l_i \\ 0 & M_2 & \frac{1}{\sqrt{2}}g_2\nu_1 & -\frac{1}{\sqrt{2}}g_2\nu_2 & \frac{1}{\sqrt{2}}g_2l_i \\ -\frac{1}{\sqrt{2}}g_1\nu_1 & \frac{1}{\sqrt{2}}g_2\nu_1 & 0 & \mu_4 & 0 \\ \frac{1}{\sqrt{2}}g_1\nu_2 & -\frac{1}{\sqrt{2}}g_2\nu_2 & \mu_4 & 0 & 0 \\ -\frac{1}{\sqrt{2}}g_1l_i & \frac{1}{\sqrt{2}}g_2l_i & 0 & 0 & 0 \end{pmatrix} \quad (4.3)$$

suggesting that the neutrino mass generated is of order $(g_1^2 + g_2^2)l_i^2/2M$, where M is some typical neutralino mass.

The simplest constraints on neutrino masses for the first generation are the direct bounds as quoted for example in reference [22]. We could also use experimental bounds on neutrinoless double beta decay, on neutrino oscillation, and from cosmology. The oscillation effects are rather complicated and we shall not consider them in this analysis except to note that the latter would give constraints on two or more R-parity violating couplings considered together, similarly to the case where the neutrino masses and mixings are generated directly from the dimensionless couplings, and that in any case products of λ s are already very tightly constrained by these effects [19, 20, 23]. In light of the complexity of our results, we shall not derive bounds as such, but instead will discover how large the typical impact of the R-parity violating couplings can be.

4.2 Generation of Sneutrino VEVs from the RGEs

Given the discussion of sneutrino VEVs above, we wish to investigate whether the RGEs can tell us anything about the likely size of such effects. The usual scenario has supersymmetry breaking in the hidden sector communicated to the visible sector only by gravity, so that the soft breaking terms take the form of trilinear and bilinear terms proportional to the corresponding Yukawa couplings and μ terms, with universal soft masses. If we make this assumption, then at the GUT scale (or perhaps more plausibly the Planck scale) we can simply rotate away the μ_i for $i \neq 4$ as described above, and in doing so we will also set all $D_i = 0$ except for D_4 without generating any non-zero $m_{H_1 L_i}^2$. Hence we shall assume that at the GUT scale we have done this, and so our initial configuration will have R-parity violation only through dimensionless couplings and trilinear terms.

If we then run our initial conditions down to the weak scale, then we will find that here sneutrino VEVs will only be generated through the following non-zero products of couplings.

$$\begin{array}{lll} \lambda_{i33} h_\tau & \text{or} & \lambda'_{i33} h_b \quad \text{generating } \mu_i, D_i, m_{H_1 L_i}^2 \\ C_{i33} h_\tau & \text{or} & C'_{i33} h_b \quad \text{generating } D_i \\ C_{i33} \eta_\tau & \text{or} & C'_{i33} \eta_b \quad \text{generating } m_{H_1 L_i}^2 \end{array} \quad (4.4)$$

These of course are exactly what we would expect, since in order to generate sneutrino VEVs we must have terms mixing L_i and H_1 , as shown in Figure 1.

Once we run down to the weak scale, however, we must perform another change of basis to that in which $\mu_i = 0$, and this will introduce additional effects. The simplest way to describe these is by recasting the relevant RGEs in the basis where we continuously rotate as we run so as to ensure that

$$\frac{d\mu_i}{dt} = 0 \quad (4.5)$$

In this basis we find that for $i \neq 4$ and assuming that the diagonal terms in the soft

mass matrices are very much greater than the off-diagonal terms and $\mu_4 \gg \mu_i$

$$\begin{aligned}
16\pi^2 \frac{dD_i}{dt} &\simeq D_i(3h_t^2 - g_1^2 - 3g_2^2) - 6C'_{i33}h_b\mu_4 - 2C_{i33}h_\tau\mu_4 \\
16\pi^2 \frac{dm_{H_1 L_i}^2}{dt} &\simeq -\lambda_{i33}h_\tau(2m_{L_i}^2 + 2m_{e_3}^2 + 2m_{L_3}^2) \\
&\quad -\lambda'_{i33}h_b(6m_{L_i}^2 + 6m_{d_3}^2 + 6m_{Q_3}^2) \\
&\quad -2C_{i33}\eta_\tau - 6C'_{i33}\eta_b
\end{aligned} \tag{4.6}$$

Note that although it is possible to cancel off some of the L_i - H_1 mixing terms by a field redefinition, not all terms can be cancelled simultaneously. Here for example the rotation has removed the m_{H_1} terms from the RGE for $m_{H_1 L_i}^2$, but increased the coefficient of the m_{L_i} terms.

We see that the effects are likely to be largest when $\tan\beta$ is large, giving large h_b and h_τ , but that the dependence is clearly rather complicated. More significantly, the sneutrino VEV will in general be proportional to the R-parity violating coupling, and hence the neutrino mass to the coupling squared.

4.3 Numerical Results

Many of the numerical methods and assumptions which we use here will be standard for calculations throughout this paper. We have as input parameters m_t , α_3 , m_0 , A_0 , $M_{1/2}$, $\tan\beta = \nu_2/\nu_1$ and the sign of μ . We run the Yukawa and gauge couplings up to the GUT scale, where we impose universality of the soft masses, but not unification, and set any R-parity violating couplings which we wish to investigate. m_0^2 and $M_{1/2}$ are the values of all the diagonal elements of the scalar soft mass-squared matrices and the universal gaugino mass respectively. We set each trilinear coupling equal to the corresponding Yukawa coupling multiplied by A_0 , so that for example $C'_{ijk}(M_{GUT}) = \lambda'_{ijk}(M_{GUT})A_0$. The masses and couplings are then run down to low energy to give output. μ_4 and D_4 are chosen so as to give the correct minimum of the one-loop

effective potential. We do not include any threshold corrections at either scale, using the non-SUSY RGEs below $M_{1/2}$ and the SUSY RGEs above it.

Typical results are shown in Figure 2a, where we set $\lambda_{133}(M_{GUT}) = 0.01$ and Figure 2b where instead we set $\lambda'_{133}(M_{GUT}) = 0.001$. Input parameters are $m_t = 175\text{GeV}$, $\alpha_3(M_Z) = 0.12$, $A_0 = 0$, $M_{1/2} = 500\text{GeV}$, and we plot the absolute magnitude of the sneutrino VEV and the corresponding neutrino mass as a function of m_{L_1} , the soft mass of the left-handed slepton, for both signs of μ and for $\tan\beta = 2, 20$. We note that in certain cases the sneutrino VEV changes sign at some value where the contributions for the non-zero D_1 and $m_{H_1 L_1}^2$ exactly cancel. It is clear from equation (4.6) that, for given A_0 and for one or other sign of μ_4 , D_1 and $m_{H_1 L_1}^2$ will have opposite sign, and here we see that complete cancellation can occur when $\mu_4 > 0$. Here larger $\tan\beta$ gives a larger sneutrino VEV and hence larger neutrino mass.

Although we might naïvely expect from the form of equation (4.3) that increasing $M_{1/2}$ (for fixed m_{L_i}) should cause the resulting neutrino mass to decrease, increasing $M_{1/2}$ also changes the value of μ_4 and affects the running of all the dimensionful parameters and so the situation is rather complicated. In Figure 3 we plot the absolute magnitude of the sneutrino VEV and the resulting neutrino mass against $M_{1/2}$ for the same parameters as Figure 2b, but with m_{L_1} held fixed at 500GeV . Again we see that the relative cancellation occurs to give zero neutrino mass for some set of input parameters, and is noticeable that even with $M_{1/2}$ as large as 500GeV , the neutrino mass is still increasing with increasing $M_{1/2}$ in at least some cases.

The effect of varying A_0 is also large, as shown in Figure 4. The main limit on the size of A_0 is that its absolute value should be less than around 3 times a typical slepton mass to avoid charge or colour breaking minima [24]. In Figure 4 we vary A_0 over the whole of this range for the same parameters as in Figure 2b, but with $m_{L_i} = M_{1/2} = 500\text{GeV}$. From this figure it is clear that the cancellation of the effect

can occur for either sign of μ , depending on the signs and relative magnitudes of the low energy value of the trilinear couplings.

We now turn to a discussion of how these calculations can be used to derive a limit on the couplings. It is clearly straightforward to derive bounds on λ_{i33} and λ'_{i33} for a point on one or other of Figures 2a to 4 by calculating which value of λ or λ' gives a neutrino mass which is acceptable in the light of the experimental limits, given that the sneutrino VEV is directly proportional to λ_{i33} (or λ'_{i33}), and so the neutrino mass generated is proportional to the square of each of the coupling. What is perhaps most interesting here is that although the constraint tends to become less tight with increasing values of the soft masses, as is generally the case for the constraints on R-parity violating couplings, the decrease can be slow relative to the case for limits derived from one-loop diagrams with internal sfermion lines, as these are almost always power-law suppressed by soft masses. We typically find that even for soft masses of order 500GeV the bounds are relatively tight, with $\lambda_{i33}(M_{GUT}) \sim 0.01$ and $\lambda'_{i33}(M_{GUT}) \sim 0.001$ both giving neutrino masses of order 1keV or more, suggesting a bound on these couplings which is at least an order of magnitude tighter for the first generation. These constraints are much tighter than those in the literature on individual couplings [9, 10, 11], since normally the tightest constraints are on products of couplings. It should however be noted that we are quoting limits on couplings at the GUT scale, which should be converted to values at the weak scale using equation (2.3) for comparison with those given by most other authors.

Such limits are obviously greatly hampered by the dependence on the many input parameters, on the assumptions about the GUT scale structure, and in particular by the fact that there are strong cancellations between terms. We note that one possible cause of partial cancellation, namely having λ_{i33} and λ'_{i33} of the same order and opposite sign, is unlikely in the context of certain GUTs, where we would typically expect $\lambda_{i33}(M_{GUT}) = \lambda'_{i33}(M_{GUT})$ just as $h_b(M_{GUT}) = h_\tau(M_{GUT})$. Hence our results

should be regarded as indicative of the likely magnitude of the effect rather than being able to strongly constrain the electroweak scale values of the couplings in isolation. Nevertheless, it is significant that the RGEs typically give such large effects, and in constructing any model which includes any of the couplings which can generate neutrino masses it is necessary either to set them extremely small or else to fine-tune away the unwanted effects.

5 $\mu \rightarrow e\gamma$

5.1 Contributions

The process $\mu \rightarrow e\gamma$ is one of the most tightly constrained examples of FCNC. Since this process cannot occur in the SM, its observation would be pressing evidence for new physics beyond the SM. Experiments [25] have calculated an upper bound on the branching ratio (BR) of

$$BR(\mu \rightarrow e\gamma) < 4.9 \times 10^{-11} \text{ at 90\% CL} \quad (5.1)$$

In SUSY models, a non-zero rate can be generated through non-diagonal slepton mass matrices [14, 26, 27], and also through the direct effects of R-parity violating couplings [3, 16, 19]. However, as noted above, R-parity violation induces LFV through soft terms, and so in any realistic model where the latter effects occur, so will the former, and here we shall consider the two effects together.

The total branching ratio for the process $\mu \rightarrow e\gamma$ can be written as:

$$BR(\mu \rightarrow e\gamma) = \frac{12\pi^2}{G_F^2} \left(|\tilde{A}_{LR}|^2 + |\tilde{A}_{RL}|^2 \right) \quad (5.2)$$

where G_F is the Fermi constant, and \tilde{A}_{LR} , \tilde{A}_{RL} are the total amplitudes to the LR and RL transitions respectively. Here

$$\tilde{A}_i = \tilde{A}_i^\lambda + \tilde{A}_i^{\lambda'} + \tilde{A}_i^{\Delta m} \quad (5.3)$$

with $i = LR, RL$ and the different terms are as follows. The various contributions to \tilde{A}_{LR}^λ , $\tilde{A}_{LR}^{\lambda'}$ and $\tilde{A}_{LR}^{\Delta m}$ are shown in Figures 5 to 7 respectively. Diagrams contributing to \tilde{A}_{RL} are not shown, but are similar to the LR case for \tilde{A}_{RL}^λ and the neutralino contributions to $\tilde{A}_{RL}^{\Delta m}$. Both $\tilde{A}_{RL}^{\lambda'}$ and the chargino contributions to $\tilde{A}_{RL}^{\Delta m}$ are proportional to the electron mass and thus neglected.

Results for the various amplitudes are :

$$\tilde{A}_{LR}^\lambda = \frac{e}{16\pi^2} \sum_{i,j=1}^3 \lambda_{i1j} \lambda_{i2j} \frac{1}{6} \left(\frac{1}{m_{\tilde{\nu}_i}^2} - \frac{1}{2} \left[\frac{\sin^2 \theta_{e_j}}{m_{\tilde{e}_j^{(1)}}^2} + \frac{\cos^2 \theta_{e_j}}{m_{\tilde{e}_j^{(2)}}^2} \right] \right), \quad (5.4)$$

where e is the electromagnetic constant, $m_{\tilde{\nu}_i}$ is the mass of the corresponding sneutrino, $m_{\tilde{e}_j^{(1),(2)}}$ denote the two mass eigenvalues of the mass matrix for the j^{th} generation of sleptons and $\sin \theta_{e_j}$, $\cos \theta_{e_j}$ are elements of the corresponding orthogonal diagonalisation matrix. These are given by:

$$\begin{aligned} \sin^2 \theta_{e_j} &= \frac{1}{2} \left(1 - \frac{m_{\tilde{e}_j^L}^2 - m_{\tilde{e}_j^R}^2}{m_{\tilde{e}_j^{(1)}}^2 - m_{\tilde{e}_j^{(2)}}^2} \right) \\ \cos^2 \theta_{e_j} &= \frac{1}{2} \left(1 + \frac{m_{\tilde{e}_j^L}^2 - m_{\tilde{e}_j^R}^2}{m_{\tilde{e}_j^{(1)}}^2 - m_{\tilde{e}_j^{(2)}}^2} \right) \end{aligned} \quad (5.5)$$

so that state $e^{(1)}$ is defined by

$$|e^{(1)}\rangle = \cos \theta_e |e_L\rangle + \sin \theta_e |e_R\rangle \quad (5.6)$$

The second amplitude is given by:

$$\begin{aligned} \tilde{A}_{LR}^{\lambda'} &= \frac{e}{16\pi^2} \sum_{i,j=1}^3 \lambda'_{i1j} \lambda'_{i2j} \left(\frac{\cos^2 \theta_{u_i}}{m_{\tilde{u}_i^{(1)}}^2} (F_1(x_{ji}^{(1)}) + 2F_2(x_{ji}^{(1)})) \right. \\ &+ \frac{\sin^2 \theta_{u_i}}{m_{\tilde{u}_i^{(2)}}^2} (F_1(x_{ji}^{(2)}) + 2F_2(x_{ji}^{(2)})) - \frac{\sin^2 \theta_{d_j}}{m_{\tilde{d}_j^{(1)}}^2} (2F_1(x_{ij}'^{(1)}) + F_2(x_{ij}'^{(1)})) \\ &\left. - \frac{\cos^2 \theta_{d_j}}{m_{\tilde{d}_j^{(2)}}^2} (2F_1(x_{ij}'^{(2)}) + F_2(x_{ij}'^{(2)})) \right). \end{aligned} \quad (5.7)$$

The various functions are mostly found in [27] and [28], and are reproduced in Appendix B for convenience, while $x_{ji}^{(1),(2)} = \frac{m_{d_j}^2}{m_{\tilde{u}_i^{(1),(2)}}^2}$, $x'_{ij}^{(1),(2)} = \frac{m_{u_i}^2}{m_{\tilde{d}_j^{(1),(2)}}^2}$.

Finally the third amplitude is:

$$\begin{aligned}
\tilde{A}_{LR}^{\Delta m} = & \frac{eg^2}{8\pi^2} \left\{ -\frac{1}{2} \frac{\Delta m_{\tilde{\nu}_e \tilde{\nu}_\mu}^2}{m_{\tilde{\nu}}^4} \sum_{j=1}^2 \left(|V_{j1}|^2 G(x_j) - \frac{V_{j1} U_{j2}}{\sqrt{2} \cos \beta} \frac{M_{\chi_j^-}}{M_W} H(x_j) \right) \right. \\
& + \frac{\Delta m_{\tilde{e}_L \tilde{\mu}_L}^2}{m_{\tilde{e}_L}^4} \sum_{j=1}^4 \left(\left| s_W N'_{j1} + \frac{1}{c_W} \left(\frac{1}{2} - s_W^2 \right) N'_{j2} \right|^2 F(x_{jL}) \right. \\
& \quad \left. - \left[s_W N'_{j1} + \frac{1}{c_W} \left(\frac{1}{2} - s_W^2 \right) N'_{j2} \right] \frac{N_{j3}}{2 \cos \beta} \frac{M_{\chi_j^0}}{M_W} L(x_{jL}) \right) \\
& + \frac{\Delta m_{\tilde{e}_L \tilde{\mu}_L}^2}{m_{\tilde{e}_L}^2 - m_{\tilde{e}_R}^2} \sum_{j=1}^4 \left[s_W N'_{j1} + \frac{1}{c_W} \left(\frac{1}{2} - s_W^2 \right) N'_{j2} \right] \left(-s_W N'_{j1} + \frac{s_W^2}{c_W} N'_{j2} \right) \\
& \times M_{\chi_j^0} (A_\mu + \mu \tan \beta) \left(\frac{1}{m_{\tilde{e}_L}^2 - m_{\tilde{e}_R}^2} \left[\frac{F_4(x_{jL})}{m_{\tilde{e}_L}^2} - \frac{F_4(x_{jR})}{m_{\tilde{e}_R}^2} \right] + \frac{L(x_{jL})}{m_{\tilde{e}_L}^4} \right) \Big\} , \tag{5.8}
\end{aligned}$$

where s_W (c_W) is the sine (cosine) of the Weinberg angle, and g is the SU(2) gauge coupling constant. Also,

$$m_{\tilde{\nu}_e}^2 = m_{\tilde{\nu}_\mu}^2 \equiv m_{\tilde{\nu}}^2, \quad m_{\tilde{e}_L}^2 = m_{\tilde{\mu}_L}^2, \quad m_{\tilde{e}_R}^2 = m_{\tilde{\mu}_R}^2, \tag{5.9}$$

and

$$x_j = \frac{M_{\chi_j^-}^2}{m_{\tilde{\nu}}^2}, \quad x_{jL} = \frac{M_{\chi_j^0}^2}{m_{\tilde{e}_L}^2}, \quad x_{jR} = \frac{M_{\chi_j^0}^2}{m_{\tilde{e}_R}^2} \tag{5.10}$$

and the mixing matrices U , V , N , N' are defined as in [29]. Finally A_μ is the trilinear coupling for the second generation of sleptons. We use $\Delta m_{\tilde{\nu}_e \tilde{\nu}_\mu}^2 = \Delta m_{\tilde{e}_L \tilde{\mu}_L}^2$ and $\Delta m_{\tilde{e}_R \tilde{\mu}_R}^2$ instead of $m_{L_1 L_2}^2$ and $m_{e_1 e_2}^2$ as in Appendix A to avoid confusion between generation and mass eigenstate labels.

The RL amplitudes are given by:

$$\tilde{A}_{RL}^\lambda = \frac{e}{16\pi^2} \sum_{i,j=1}^3 \lambda_{ij1} \lambda_{ij2} \frac{1}{6} \left(\frac{1}{m_{\tilde{\nu}_i}^2} - \frac{1}{2} \left[\frac{\cos^2 \theta_{e_j}}{m_{\tilde{e}_j^{(1)}}^2} + \frac{\sin^2 \theta_{e_j}}{m_{\tilde{e}_j^{(2)}}^2} \right] \right), \tag{5.11}$$

with $\tilde{A}_{RL}^{\lambda'} = 0$ and:

$$\tilde{A}_{RL}^{\Delta m} = \frac{eg^2}{8\pi^2} \left\{ \frac{\Delta m_{\tilde{e}_R \tilde{\mu}_R}^2}{m_{\tilde{e}_R}^4} \sum_{j=1}^4 \left(\left| -s_W N'_{j1} + \frac{s_W^2}{c_W} N'_{j2} \right|^2 F(x_{jR}) \right. \right.$$

$$\begin{aligned}
& - \left[-s_W N'_{j1} + \frac{s_W^2}{c_W} N'_{j2} \right] \frac{N'_{j3}}{2 \cos \beta} \frac{M_{\chi_j^0}}{M_W} L(x_{jR}) \Bigg) \\
& + \frac{\Delta m_{\tilde{e}_R \tilde{\mu}_R}^2}{m_{\tilde{e}_R}^2 - m_{\tilde{e}_L}^2} \sum_{j=1}^4 \left(-s_W N'_{j1} + \frac{s_W^2}{c_W} N'_{j2} \right) \left(s_W N'_{j1} + \frac{1}{c_W} \left(\frac{1}{2} - s_W^2 \right) N'_{j2} \right) \\
& \times M_{\chi_j^0} (A_\mu + \mu \tan \beta) \left(\frac{1}{m_{\tilde{e}_R}^2 - m_{\tilde{e}_L}^2} \left[\frac{F_4(x_{jR})}{m_{\tilde{e}_R}^2} - \frac{F_4(x_{jL})}{m_{\tilde{e}_L}^2} \right] + \frac{L(x_{jR})}{m_{\tilde{e}_R}^4} \right) \Bigg\}
\end{aligned} \tag{5.12}$$

In calculating these amplitudes, we have adopted the usual approximation that the electron mass is negligible relative to the muon mass, and we work to first order in both m_μ/M_W and $m_\mu(A_\mu + \mu \tan \beta)/(m_{\tilde{e}_L}^2 - m_{\tilde{e}_R}^2)$.

Finally we note that we have neglected many diagrams which are suppressed by the mixing between neutralinos and neutrinos, or between charginos and charged leptons [3, 16]. Two typical examples of such diagrams contributing to \tilde{A}_{LR} are shown in Figure 8. Such terms will exist due to mixing of neutral fermions as shown by the mass matrix of equation (4.3), and similarly from the mass matrix for charginos and sleptons which contributes to the lagrangian (in two-spinor notation)

$$(-i\tilde{W}^-, \tilde{H}_1^-, e_{Li}) \begin{pmatrix} M_2 & g_2 \nu_2 & 0 \\ g_2 \nu_1 & \mu_4 & h_i l_i \\ g_2 l_i & 0 & h_i \nu_1 \end{pmatrix} \begin{pmatrix} -i\tilde{W}^+ \\ \tilde{H}_2^+ \\ e_{Ri}^c \end{pmatrix} \tag{5.13}$$

Here we have presented only one generation for simplicity, and h_i is its mass-generating Yukawa coupling. However, even for the third generation the sneutrino VEV l_i must be quite small to avoid an excessive neutrino mass, and hence the mixing is small. Relative to the direct λ^2 proportional contributions shown in Figure 5 such diagrams with a predominantly lepton line are suppressed by $g_2^2 l_i/(\lambda M)$ (where a factor g_2/λ is from the differing couplings, and $g_2 l_i/M$ is from the mixing angle). Thus we expect this diagram to contribute less than the direct contribution except when λ is so small that both are negligible, in which case we would anyway not expect the generation of large l_i , since from our earlier discussion of sneutrino VEVs we always have $l_i < \lambda M$ by at least an order of magnitude. Similarly, if the internal fermion line is predominantly neutralino or chargino, such contributions are similar to those shown in Figure 7 but suppressed by a relative factor $l_i \lambda/M$, and so negligible.

Further diagrams can be drawn with mixing between sneutrinos and neutral Higgs states, and between charged sleptons and charged Higgs states, but by similar arguments we are justified in neglecting those too. We note however that although we expect such diagrams to give weaker bounds than for the case where corresponding diagrams without sneutrino VEV insertions exist, they can provide very weak constraints on products of couplings which we cannot otherwise bound. For example Figure 8a will allow a bound on the product $\lambda_{i33}\lambda_{12i}$.

5.2 Analytical Discussion

Given the complexity of the expressions shown above, we can try to see whether in certain limits we are able to derive analytical bounds on the R-parity violating couplings. In each case, we shall set only two R-parity violating dimensionless couplings non-zero at M_{GUT} and see what effects they generate. We begin by discussing the relatively simple “direct” contributions to \tilde{A}^λ and $\tilde{A}^{\lambda'}$ before turning to the “indirect” contributions of $\tilde{A}^{\Delta m}$.

Due to the antisymmetry of the λ_{ijk} couplings with respect to the first two indices, we will always have $i = 3$ in equation (5.4) and therefore $m_{\tilde{\nu}_i} = m_{\tilde{\nu}_\tau}$. Also note that, for the first two generations, the weak interaction and the mass eigenstates are practically the same, so we can take then $\sin^2 \theta_{e_k} = 0$, $\cos^2 \theta_{e_k} = 1$ and also $m_{\tilde{e}_k^{(1),(2)}}^2 = m_{\tilde{e}_k^{L,R}}^2$, with $k = 1, 2$. This gives us a bound on products of λ s at the low-energy scale

$$|\lambda_{31k}(M_Z)\lambda_{32k}(M_Z)| < 4.6 \times 10^{-4} \left(\frac{m}{100\text{Gev}} \right)^2 \quad k = 1, 2, \quad (5.14)$$

assuming that $m_{\tilde{\nu}_\tau} \simeq m_{\tilde{e}_R} \simeq m$. Bounds for the case $k = 3$ are pretty similar to these, though their dependence on the mixing in the stau sector makes them less straightforward. However in the case of maximal mixing (that is, $\sin^2 \theta_\tau = \cos^2 \theta_\tau = \frac{1}{2}$,

and with one stau very much lighter than the other) we can see that:

$$|\lambda_{313}(M_Z)\lambda_{323}(M_Z)| < 2.3 \times 10^{-4} \left[\left(\frac{100\text{Gev}}{m_{\tilde{\nu}_\tau}} \right)^2 - \left(\frac{100\text{Gev}}{2m_{\tilde{\tau}_2}} \right)^2 \right]^{-1}, \quad (5.15)$$

where $m_{\tilde{\tau}_2}$ is the lighter stau mass eigenvalue. Therefore we see that there is a possibility of cancellation inside the bracket, thus considerably reducing the branching ration generated by this process and hence relaxing the bound. A further problem with these analytical limits on slepton mediated diagrams is that we are assuming that the right and left handed sleptons have the same masses, and in practice this assumption can break down completely, as will become apparent when we come to consider our exact numerical results.

We turn now to possible limits on these couplings coming from the RL contributions to $\mu \rightarrow e\gamma$ given in eq. (5.4). In this case we have one pair λ_{ij1} , λ_{ij2} , with $i, j = 1, 2$, and $i \neq j$ which satisfy the bound

$$|\lambda_{ij1}(M_Z)\lambda_{ij2}(M_Z)| < 2.3 \times 10^{-4} \left(\frac{m}{100\text{Gev}} \right)^2 \quad i, j = 1, 2, \quad (5.16)$$

Note that there is a relative factor of two between equations (5.14) and (5.16) from the fact that we must set $\lambda_{ij1} = -\lambda_{ji1}$ and so cannot set only one $\lambda \neq 0$ at once. The remaining cases, $i = 3, j = 1, 2$, allow cancellations in a similar way to the case of equation (5.15).

Concerning the λ' couplings, we can turn back to eq. (5.7) and notice that for $i, j = 1, 2$ again the weak interaction and mass eigenstates are the same, so that $\sin^2 \theta_{u_i} = \sin^2 \theta_{d_j} = 0$, $\cos^2 \theta_{u_i} = \cos^2 \theta_{d_j} = 1$ and $m_{\tilde{u}_i^{(1),(2)}}^2 = m_{\tilde{u}_i^{L,R}}^2$, $m_{\tilde{d}_j^{(1),(2)}}^2 = m_{\tilde{d}_j^{L,R}}^2$. Furthermore, due to the small values of the quark masses for these first two generations, x_{ji} and x'_{ij} are very small as well, and $F_1(x)$, $F_2(x)$ can be replaced by $1/6$, $1/12$ respectively. All this allows us to deduce that

$$|\lambda'_{1ij}(M_Z)\lambda'_{2ij}(M_Z)| < 4.6 \times 10^{-4} \left(\frac{m}{100\text{Gev}} \right)^2 \quad i, j = 1, 2 \quad (5.17)$$

where here we assume that the squark masses are degenerate at m . However when either i, j or both are equal to 3, everything is going to depend on the mixing between stops and/or sbottoms; in that case we find a tighter bound (a factor of 2 smaller than for the other couplings) when that mixing is large by assuming that the contribution of the lightest mass eigenvalue (sbottom for $i = 1, 2$ and $j = 3$, and stop for the rest) will be the dominant one in the corresponding amplitude.

So far we have presented analytical bounds on products of couplings at the electroweak scale. However, note that these can immediately be translated into bounds on the same couplings at M_{GUT} , just by performing the corresponding running up from M_Z . Moreover, the approximate solutions to the RGEs sketched in eq.(2.3) will provide the reader with automatic bounds for most of the relevant cases.

By looking at eqs. (5.8), (5.12) it is clear that not much can be extracted from them analytically except in limits so simple as not to be useful. However, we can at least remark upon their sign and order of magnitude. If we consider the corresponding RGEs for LFV with diagonal mass terms dominant,

$$16\pi^2 \frac{dm_{e_i e_j}^2}{dt} = \sum_{mn} \left(\lambda_{mni} \lambda_{mnj} (m_{e_i}^2 + m_{e_j}^2 + 4m_{L_n}^2) + 2C_{mni} C_{mnj} \right) \quad (5.18)$$

$$\begin{aligned} 16\pi^2 \frac{dm_{L_i L_j}^2}{dt} = & \sum_{mn} \left(\lambda_{imn} \lambda_{jmn} (m_{L_i}^2 + m_{L_j}^2 + 2m_{e_n}^2 + 2m_{L_m}^2) \right. \\ & \left. + 2C_{imn} C_{jmn} \right) \\ & + \sum_{mn} \left(3\lambda'_{imn} \lambda'_{jmn} (m_{L_i}^2 + m_{L_j}^2 + 2m_{d_n}^2 + 2m_{Q_m}^2) \right. \\ & \left. + 6C'_{imn} C'_{jmn} \right) , \end{aligned} \quad (5.19)$$

we can solve these equations only in the limit where we only consider the contributions from the largest gauge coupling after imposing unification at M_{GUT} . However, it is more useful simply to give the empirical results below :

$$m_{e_i e_j}^2(M_Z) = - \sum_{mn} \lambda_{mni} \lambda_{mnj}(M_{GUT}) (1.7m_0^2 + 0.6M_{1/2}^2 - 0.3A_0 M_{1/2} + 0.6A_0^2)$$

$$\begin{aligned}
m_{L_i L_j}^2(M_Z) = & - \sum_{mn} \lambda_{imn} \lambda_{jmn} (M_{GUT}) (1.7m_0^2 + 0.6M_{1/2}^2 - 0.3A_0 M_{1/2} + 0.6A_0^2) \\
& + \sum_{mn} \lambda'_{imn} \lambda'_{jmn} (M_{GUT}) (15m_0^2 + 30M_{1/2}^2 - 20A_0 M_{1/2} + 5A_0^2) \quad (5.20)
\end{aligned}$$

The accuracy of these formulae is roughly at the 10% level for the case where we deal with λ only, but is much lower for the case with λ' due to the strong dependence on the QCD coupling, whose value is uncertain and which typically appears in the RGEs with larger coefficients. In the latter case we find that the $M_{1/2}^2$ coefficient can vary by almost a factor of two, and so the results should be regarded as merely indicative of the likely scale of the terms generated.

Hence we see that the terms $\Delta m_{\tilde{e}_L \tilde{\mu}_L}^2 / m_{\tilde{e}_L}^2$ and $\Delta m_{\tilde{e}_R \tilde{\mu}_R}^2 / m_{\tilde{e}_R}^2$ are of the same order as $\lambda_{1ij} \lambda_{2ij} + 3\lambda'_{1ij} \lambda'_{2ij}$ and $\lambda_{ij1} \lambda_{ij2}$ respectively where the couplings are taken at M_Z , and are rather larger when we have non-zero λ' s than λ s. Given the range of values of the various functions and the other couplings, it is then straightforward to check that we expect the neutralino and chargino contributions can be at least comparable in magnitude to the direct contributions, and often larger, particularly for the case of the λ' where the internal particles in the loop for the direct case are heavier but the impact from Δm^2 is larger than for the λ case.

We also note that except $H(x) > G(x)$, $L(x) > F(x)$, and hence if all the mixing matrix elements are significant we expect the second term in each of the chargino and neutralino contributions to dominate. Thus we might expect that usually $\tilde{A}^{\Delta m}$ will grow with increasing $\tan \beta$, and fall off only slowly with increasing chargino and neutralino masses, since the explicit mass factor will partially cancel the dependency in the function.

Another important point which we should make here is that when we add up all the contributions to \tilde{A}_{LR} from equations (5.4), (5.7), and (5.8), and to \tilde{A}_{RL} from (5.11) and (5.12), to obtain the total, there are likely to be cancellations. For example, if we consider $\lambda_{i1j} \lambda_{i2j} > 0$ in the limit where there is very little gaugino-higgsino mixing,

then the contributions to \tilde{A}_{LR}^λ and the first chargino term of $\tilde{A}_{LR}^{\Delta m}$ are both positive, while the contribution to the first neutralino contribution to $\tilde{A}_{LR}^{\Delta m}$ is negative, and other terms will vanish.

5.3 Numerical Results

In any case, we can derive through these equations new bounds on products of λ and λ' . As discussed above for the sneutrino VEV calculation, we simply impose unification at M_{GUT} with some pair of R-parity couplings non-zero, evolve down to low energy and then investigate the amplitudes for $\mu \rightarrow e\gamma$. Given that here there will be sensitivity to virtually every parameter through the complicated dependence on the spectrum, we shall attempt to pick typical scenarios and examine whether reasonable conclusions can be drawn.

Firstly, let us consider the impact of $\lambda'_{111}(M_{GUT}) = \lambda'_{211}(M_{GUT}) = 0.001$. Here we note that we expect λ'_{i33} to be negligible because of its generically very large impact on sneutrino VEVs and hence neutrino masses as discussed above, while we shall avoid λ'_{1i3} and λ'_{13i} for simplicity. For $m_0 = M_{1/2} = 100\text{GeV}$, we expect that the values chosen will give a contribution to the amplitude which is less than the experimental limit by about two orders of magnitude using Eq. (5.17).

We show the resulting contributions to the amplitude as a function of $M_{1/2}$ in Figure 9. Here we have set $\tan\beta = 10$, $m_0 = 100\text{GeV}$, $A_0 = 0$, $\mu_4 > 0$, and $\lambda'_{111}(M_{GUT}) = \lambda'_{211}(M_{GUT}) = 0.001$. What is remarkable about this figure is that it is clear that in this case the direct contributions are completely negligible relative to those from the chargino and neutralino mediated diagrams. Similarly keeping $M_{1/2} = 100\text{GeV}$, so that the chargino is always light, and varying m_0 , we find contributions of form of Figure 10. Here we find a curious cancellation between neutralino diagrams, so that the neutralino contribution at one point changes sign relative to the chargino

contribution, but is in any case always small. Finally we show the dependence on A_0 in Figure 11. Naturally, the direct contribution to the amplitude is independent of A_0 (up to the very slight dependence of the squark spectrum), but since altering A_0 can affect the chargino and neutralino spectra by altering the values of μ and B which give the correct electroweak breaking and also affect the running of the off-diagonal mass terms, it can have a significant impact on the indirect contributions.

We now touch upon how sensitive these results are to the other parameters. Selecting $\mu_4 < 0$ gives a lighter chargino, which in general increases the chargino dominated rate, but in practice we find that since to evade the experimental chargino bound we must then pick higher values for the soft masses m_0 and $M_{1/2}$, this does not in fact lead to very different behaviour.

Increasing $\tan\beta$ can both directly enhance the contributions from diagrams with a helicity flip on the chargino or neutralino line and also change the spectra in a complicated way directly and through μ_4 . In fact, the first of these effects seems most important, as seen in Figure 12, which is similar to Figure 9, but with $\tan\beta$ set to 30. Here the chargino and neutralino contributions both increase by around a factor of three, as we would expect if the dominant contribution to these is via higgsino-neutralino mixed states.

In conclusion of our discussion of the effects generated by a pair of λ' couplings, we have found that the dominant contribution to the amplitude is that of the chargino followed closely by that of the neutralino, with the direct contribution from the squark mediated diagrams almost completely negligible. This clearly has important implications in any attempt to bound R-parity violating couplings, since the only case where we can do a reasonably complete analytical analysis is irrelevant. In general, we can conclude that a choice of $\lambda'_{1ij}\lambda'_{2ij}(M_{GUT})$ of order 10^{-6} is fairly safe for m_0 and $M_{1/2}$ of order 100GeV, compared to a limit from the direct diagrams about two orders of

magnitude weaker. However, the various contributions are sufficiently complicated that this can only really be regarded as an order of magnitude estimate, which may be evaded by appropriate choice of $\tan\beta$ and the various soft parameters. We emphasise here that the amplitudes \tilde{A} are all directly proportional to the product of the two couplings, and as before it is straightforward to convert our figures showing the amplitude into bounds for a given point in parameter space.

Having shown the general behaviour for the λ' case, we now consider two alternative scenarios. Firstly, we consider the case $\lambda_{131}(M_{GUT}) = \lambda_{231}(M_{GUT}) = 0.01$. Here we note that these couplings are sufficiently large to give a direct contribution which is close to the present experimental limit.

We show the resulting contributions to the amplitude as a function of $M_{1/2}$ in Figure 13, with $\tan\beta = 10$, $m_0 = 100\text{GeV}$, $A_0 = 0$, $\mu_4 > 0$, and $\lambda_{131}(M_{GUT}) = \lambda_{231}(M_{GUT}) = 0.01$. The apparently pathological behaviour of the direct contribution, which changes sign even though it does not depend on the stau masses and mixings, can be understood as follows. From equation (5.4), we see that the amplitude behaves as

$$\tilde{A}_{LR}^\lambda \sim \frac{1}{m_{\tilde{\nu}_\tau}^2} - \frac{1}{2m_{\tilde{e}_R}^2} \quad (5.21)$$

For small $M_{1/2}$, the slepton and sneutrino masses will be similar, and so the first term on the right hand side of this equation will be larger and the result positive; however as we increase $M_{1/2}$, $m_{\tilde{\nu}_\tau}^2$ will grow larger than $2m_{\tilde{e}_R}^2$ due to its greater electroweak radiative corrections in the RGEs, at which point the amplitude changes sign. We find this behaviour occurring when $m_{\tilde{\nu}_\tau}$ and $m_{\tilde{e}_R}$ are around 230GeV and 165GeV respectively. Here, however, the chargino and neutralino contributions are still larger than that of the direct contribution, although much less so than in the case of the λ' diagrams.

In Figure 14 we show the same data as for Figure 13 except for $\tan\beta = 2$, but with

$M_{1/2}$ held constant at 100GeV, and varying A_0 . This is an example of exact cancellation of the amplitude. Since we often find that the direct and indirect contributions to the amplitude are of similar magnitude and opposite sign, there are many cases where the cancellation can be very good, particularly if $\tan \beta$ is not too large (since if we increase $\tan \beta$ we increase the chargino and neutralino mediated contributions to the amplitude without greatly changing the slepton mediated contributions).

Hence, our conclusion for the contribution to $\mu \rightarrow e\gamma$ from setting $\lambda_{131}\lambda_{231}$ non-zero is ultimately that the new contributions from chargino and neutralino mediated diagrams dominate for large $\tan \beta$, but that there are some fairly subtle cancellations which become increasingly significant for smaller $\tan \beta$. Often the direct and indirect contributions have opposite sign, and hence it is not really possible to derive a reliable bound.

The last scenario which we shall consider is that of \tilde{A}_{RL} , which we generate by setting $\lambda_{121}(M_{GUT}) = \lambda_{122}(M_{GUT}) = 0.01$. Again, we expect the contributions from the direct diagrams to be relatively close to the experimental limit. However, this case is rather different from the two previous ones because we no longer have a chargino contribution. Hence we would expect that the cancellations between direct and indirect effects might occur for larger $\tan \beta$. That this is the case is shown in Figure 15, in which we show the amplitude as a function of $M_{1/2}$ with again $\tan \beta = 10$, $m_0 = 100\text{GeV}$, $A_0 = 0$, $\mu_4 > 0$, and $\lambda_{121}(M_{GUT}) = \lambda_{122}(M_{GUT}) = 0.01$, showing that the cancellation ensures that the amplitude remains well below the experimental limit.

We conclude this section by summarising our results. Firstly, we find rather different behaviour for the three different scenarios which we have considered. For the λ' case, the chargino and neutralino mediated diagrams with flavour violation through soft mass insertions dominate completely the direct contributions, giving very much tighter constraints, particularly for large $\tan \beta$. For the LR effects due to λ couplings

we find again that the chargino contribution dominates, but not overwhelmingly, and there can be large cancellations. For the RL case there are no chargino contributions, and the neutralino and direct effects are usually of comparable size and opposite sign. In all of these cases it is very hard to do much more than gain an idea of the likely size of the effects in question since the parameter space is complicated, but it is clear that the $\lambda_{13i}\lambda_{23i}$ and especially $\lambda'_{1ij}\lambda'_{2ij}$ amplitudes will be much greater than those from the direct contributions alone, while the neutralino contributions to $\lambda_{ij1}\lambda_{ij2}$ are of the same order of magnitude as the direct effects. However, since there are so many possible cancellations between terms, it is essentially impossible to derive concrete bounds. The strongest reasonable statement is that, for the values we have considered for pairs of couplings at M_{GUT} of $\lambda\lambda \simeq 10^{-4}$ and $\lambda'\lambda' \simeq 10^{-6}$ we expect contributions of order the experimental limit for a very light spectrum, with the branching ratio scaling as λ^4 or λ'^4 .

6 Conclusion

In this paper we have given full RGEs for the MSSM with R-parity violation with the inclusion of all soft terms as well as all dimensionless couplings. We have given solutions to these equations for small R-parity violating couplings to relate values at the unification scale to those at low energy, and given the triviality bounds on couplings.

The inclusion of R-parity violation in our superpotential through dimensionless terms allows the generation of lepton-Higgs mixing which leads to sneutrino VEVs and hence neutrino masses. We have presented a detailed discussion of sneutrino VEV generation, together with a calculation assuming universal soft terms respecting lepton number at the unification scale. This shows that the indirect generation of sneutrino VEVs through the running of the RGEs for the soft terms often leads to

larger effects than those derived directly from one loop diagrams, and hence that λ_{133} , λ_{233} , λ'_{i33} must all be small. Typically we find that values of λ_{i33} and λ'_{i33} of order 10^{-2} and 10^{-3} at the GUT scale give masses to the corresponding neutrino of order hundreds to thousands of eV, although the exact value is quite dependent on the unification scale parameters.

Similarly, R-parity violation at the unification scale can generate large lepton and quark flavour violation both directly through one loop diagrams and indirectly through the generation of off-diagonal soft masses and hence flavour violation in the scalar sector. We have studied the process $\mu \rightarrow e\gamma$, which we have shown to be very strongly affected by chargino and neutralino mediated diagrams. These typically dominate the direct contributions which had already been calculated, typically by several orders of magnitude for the case of the λ' couplings, but there are often cancellations so that it is not possible to give precise bounds on the couplings from such processes. However, unless we invoke arbitrary cancellations, the typical size of such indirect effects on FCNC are likely to be the dominant constraint on the building of a model with non-zero R-parity violating couplings.

Our main conclusion from both these calculations is that R-parity violation can generate large lepton flavour and lepton number violating effects through the running of the dimensionful RGEs, and that these effects are often much larger than those which are generated directly by the couplings themselves. However, it is virtually impossible to turn this statement into hard numerical bounds because of the number of free input parameters and the large cancellations between different contributions.

Acknowledgements

We would like to thank Roger Phillips and Mike Berger for discussing their work of reference [8]. BdC thanks J.R. Espinosa for very enlightening discussions. PLW is very grateful to the University of Sussex for their hospitality during the final stages

of this work. The work of BdC was supported by a PPARC Postdoctoral Fellowship.

A Renormalisation Group Equations

We now present our conventions and RG equations. The superpotential and soft potential are given by

$$\begin{aligned}
W &= h_t Q_3 H_2 u_3 + h_b Q_3 H_1 d_3 + h_\tau L_3 H_1 e_3 \\
&\quad + \frac{1}{2} \lambda_{ijk} L_i L_j e_k + \lambda'_{ijk} L_i Q_j d_k + \frac{1}{2} \lambda''_{ijk} u_i d_j d_k \\
&\quad + \mu_4 H_1 H_2 + \mu_i L_i H_2 \\
V_{\text{soft}} &= \eta_t Q_3 H_2 u_3 + \eta_b Q_3 H_1 d_3 + \eta_\tau L_3 H_1 e_3 + h.c. \\
&\quad + \frac{1}{2} C_{ijk} L_i L_j e_k + C'_{ijk} L_i Q_j d_k + \frac{1}{2} C''_{ijk} u_i d_j d_k + h.c. \\
&\quad + \frac{1}{2} M_a \lambda_a^c \lambda_a + \sum_{a,b} m_{ab}^2 \varphi_a \bar{\varphi}_b \\
&\quad + D_4 H_1 H_2 + D_i L_i H_2 + h.c.
\end{aligned} \tag{A.1}$$

Here the notation is conventional, with the exception that we do not write the trilinear terms as $A \times \text{coupling}$ since this is not convenient algebraically in the context of R-parity violation, and similarly we do not write the bilinear soft term as $B\mu$. It should be noted that we now label μ as μ_4 so as to make clear the analogy between the R-parity violating bilinear terms μ_i and μ_4 . Indices indicate generation, and all gauge indices are suppressed. Raising and lowering generation indices has no particular significance. In our expressions we will use μ interchangeably with μ_4 and A_μ for η_μ/h_μ , and we express the mass eigenstates as $\tilde{e}^{(1)}$, $\tilde{e}^{(2)}$, and similarly for quarks.

The derivation of the RG equations is straightforward using standard techniques found for example in [24, 30]. Here, we use the convention that all indices which do not appear on the left hand side of the equations are summed over for the three generations, and we define

$$\xi = \sum_a Y_a g_1^2 m_{aa}^2 \tag{A.2}$$

where the sum is over all particles, and must include all appropriate degrees of freedom factors from, for example, colour and generation. Weak hypercharge is here normalised so that $Y_Q = 1/6$. We use $t = \ln \mu$, where μ is the \overline{MS} renormalisation scale.

$$\begin{aligned}
16\pi^2 \frac{dh_t}{dt} &= h_t(6h_t^2 + h_b^2 + \lambda'_{m3n}{}^2 + \lambda''_{3mn}{}^2) \\
&\quad - h_t\left(\frac{13}{9}g_1^2 + 3g_2^2 + \frac{16}{3}g_3^2\right) \\
16\pi^2 \frac{dh_b}{dt} &= h_b(6h_b^2 + h_t^2 + h_\tau^2 + 3\lambda'_{m33}{}^2 + \lambda'_{m3n}{}^2 + 2\lambda'_{mn3}{}^2 + 2\lambda''_{mn3}{}^2) \\
&\quad + h_\tau \lambda_{m33} \lambda'_{m33} - h_b\left(\frac{7}{9}g_1^2 + 3g_2^2 + \frac{16}{3}g_3^2\right) \\
16\pi^2 \frac{dh_\tau}{dt} &= h_\tau(4h_\tau^2 + 3h_b^2 + \lambda_{m33}^2 + \lambda_{m3n}^2 + \lambda_{mn3}^2 + 3\lambda'_{3mn}{}^2) \\
&\quad + 3h_b \lambda_{m33} \lambda'_{m33} - h_\tau(3g_1^2 + 3g_2^2)
\end{aligned} \tag{A.3}$$

$$\begin{aligned}
16\pi^2 \frac{d\lambda_{ijk}}{dt} &= \lambda_{lmn}(\lambda_{imn}\lambda_{ljk} + \lambda_{imk}\lambda_{ljn} + \lambda_{ijn}\lambda_{lmk}) \\
&\quad + \lambda'_{lmn}(3\lambda_{ljk}\lambda'_{imn} + 3\lambda_{ilk}\lambda'_{jmn}) \\
&\quad + \lambda_{ijk}h_\tau^2(\delta_{i3} + \delta_{j3} + 2\delta_{k3} + \delta_{j3}\delta_{k3} + \delta_{i3}\delta_{k3}) \\
&\quad + h_b h_\tau(3\delta_{j3}\delta_{k3}\lambda'_{i33} - 3\delta_{i3}\delta_{k3}\lambda'_{j33}) \\
&\quad - \lambda_{ijk}(3g_1^2 + 3g_2^2) \\
16\pi^2 \frac{d\lambda'_{ijk}}{dt} &= \lambda'_{lmn}(3\lambda'_{imn}\lambda'_{ljk} + 2\lambda'_{ijn}\lambda'_{lmk} + \lambda'_{imk}\lambda'_{ljn}) \\
&\quad + \lambda_{lmn}\lambda'_{ljk}\lambda_{imn} + 2\lambda''_{lmn}\lambda'_{ijn}\lambda''_{lmk} \\
&\quad + \lambda'_{ijk}(\delta_{i3}h_\tau^2 + \delta_{j3}h_t^2 + \delta_{j3}h_b^2 + 2\delta_{k3}h_b^2 + 3\delta_{j3}\delta_{k3}h_b^2) + \delta_{j3}\delta_{k3}h_b h_\tau \lambda_{i33} \\
&\quad - \lambda'_{ijk}\left(\frac{7}{9}g_1^2 + 3g_2^2 + \frac{16}{3}g_3^2\right) \\
16\pi^2 \frac{d\lambda''_{ijk}}{dt} &= \lambda''_{lmn}(\lambda''_{imn}\lambda''_{ljk} + 2\lambda''_{imk}\lambda''_{ljn} + 2\lambda''_{ijn}\lambda''_{lmk}) \\
&\quad + \lambda'_{lmn}(2\lambda''_{ink}\lambda'_{lmj} + 2\lambda''_{ijn}\lambda'_{lmk}) \\
&\quad + \lambda''_{ijk}(2\delta_{i3}h_t^2 + 2\delta_{j3}h_b^2 + 2\delta_{k3}h_b^2) \\
&\quad - \lambda''_{ijk}\left(\frac{4}{3}g_1^2 + 8g_3^2\right)
\end{aligned} \tag{A.4}$$

$$\begin{aligned}
16\pi^2 \frac{d\eta_t}{dt} &= \eta_t(18h_t^2 + h_b^2 + \lambda'_{m3n}{}^2 + \lambda''_{3mn}{}^2) \\
&\quad + h_t(2h_b\eta_b + 2\lambda'_{m3n}C'_{m3n} + 2\lambda''_{3mn}C''_{3mn}) \\
&\quad - \eta_t\left(\frac{13}{9}g_1^2 + 3g_2^2 + \frac{16}{3}g_3^2\right) + 2h_t\left(\frac{13}{9}g_1^2 M_1 + 3g_2^2 M_2 + \frac{16}{3}g_3^2 M_3\right)
\end{aligned}$$

$$\begin{aligned}
16\pi^2 \frac{d\eta_b}{dt} &= \eta_b(18h_b^2 + h_\tau^2 + h_t^2 + 6\lambda'_{m33}{}^2 + 2\lambda'_{mn3}{}^2 + \lambda'_{m3n}{}^2 + 2\lambda''_{mn3}{}^2) \\
&\quad + \eta_\tau(2h_b h_\tau + 2\lambda_{m33}\lambda'_{m33}) + 2h_b h_t \eta_t + C'_{m33}(3h_b \lambda'_{m33} + h_\tau \lambda_{m33}) \\
&\quad + 4h_b \lambda'_{mn3} C'_{mn3} + 2h_b \lambda'_{m3n} C'_{m3n} + 4h_b \lambda''_{mn3} C''_{mn3} \\
&\quad - \eta_b(\frac{7}{9}g_1^2 + 3g_2^2 + \frac{16}{3}g_3^2) + 2h_b(\frac{7}{9}g_1^2 M_1 + 3g_2^2 M_2 + \frac{16}{3}g_3^2 M_3) \\
16\pi^2 \frac{d\eta_\tau}{dt} &= \eta_\tau(12h_\tau^2 + 3h_b^2 + 2\lambda_{m33}^2 + \lambda_{m3n}^2 + \lambda_{mn3}^2 + 3\lambda'_{3mn}{}^2) \\
&\quad + \eta_b(6h_\tau h_b + 6\lambda_{m33}\lambda'_{m33}) + C_{m33}(3h_b \lambda'_{m33} + h_\tau \lambda_{m33}) \\
&\quad + 2h_\tau \lambda_{m3n} C_{m3n} + 2h_\tau \lambda_{mn3} C_{mn3} + 6h_\tau \lambda'_{3mn} C'_{3mn}) \\
&\quad - \eta_\tau(3g_1^2 + 3g_2^2) + 2h_\tau(3g_1^2 M_1 + 3g_2^2 M_2) \\
16\pi^2 \frac{dC_{ijk}}{dt} &= \lambda_{lmn}(\lambda_{imn}C_{ljk} + \lambda_{ljn}C_{imk} + \lambda_{lmk}C_{ijn} \\
&\quad + 2\lambda_{ijn}C_{lmk} + 2\lambda_{ljk}C_{imn} + 2\lambda_{imk}C_{ljn}) \\
&\quad + \lambda'_{lmn}(3\lambda'_{imn}C_{ljk} + 3\lambda'_{jmn}C_{ilk} + 6\lambda_{ljk}C'_{imn} + 6\lambda_{ilk}C'_{jmn}) \\
&\quad + C_{ijk}h_\tau^2(\delta_{i3} + \delta_{j3} + 2\delta_{k3} + 2\delta_{j3}\delta_{k3} + 2\delta_{i3}\delta_{k3}) \\
&\quad + \lambda_{ijk}h_\tau\eta_\tau(2\delta_{i3} + 2\delta_{j3} + 4\delta_{k3} + \delta_{j3}\delta_{k3} + \delta_{i3}\delta_{k3}) \\
&\quad + h_b\eta_\tau(3\delta_{j3}\delta_{k3}\lambda'_{i33} - 3\delta_{i3}\delta_{k3}\lambda'_{j33}) \\
&\quad + 2h_b h_\tau(3\delta_{j3}\delta_{k3}C'_{i33} - 3\delta_{i3}\delta_{k3}C'_{j33}) \\
&\quad - C_{ijk}(3g_1^2 + 3g_2^2) + 2\lambda_{ijk}(3g_1^2 M_1 + 3g_2^2 M_2) \\
16\pi^2 \frac{dC'_{ijk}}{dt} &= \lambda'_{lmn}(3\lambda'_{imn}C'_{ljk} + \lambda'_{ljn}C'_{imk} + 2\lambda'_{lmk}C'_{ijn} \\
&\quad + 4\lambda'_{ijn}C'_{lmk} + 2\lambda'_{imk}C'_{ljn} + 6\lambda'_{ljk}C'_{imn}) \\
&\quad + \lambda_{lmn}(\lambda_{imn}C'_{ljk} + 2\lambda'_{ljk}C_{imn}) \\
&\quad + \lambda''_{lmn}(2\lambda''_{lmk}C'_{ijn} + 4\lambda'_{ijn}C''_{lmk}) \\
&\quad + C'_{ijk}(\delta_{i3}h_\tau^2 + \delta_{j3}h_t^2 + \delta_{j3}h_b^2 + 2\delta_{k3}h_b^2 + 6\delta_{j3}\delta_{k3}h_b^2) \\
&\quad + \lambda'_{ijk}(2\delta_{i3}h_\tau\eta_\tau + 2\delta_{j3}h_t\eta_t + 2\delta_{j3}h_b\eta_b + 4\delta_{k3}h_b\eta_b + 3\delta_{j3}\delta_{k3}h_b\eta_b) \\
&\quad + (\delta_{j3}\delta_{k3}h_\tau\lambda_{i33}\eta_b + 2\delta_{j3}\delta_{k3}h_b h_\tau C_{i33}) \\
&\quad - C'_{ijk}(\frac{7}{9}g_1^2 + 3g_2^2 + \frac{16}{3}g_3^2) + 2\lambda'_{ijk}(\frac{7}{9}g_1^2 M_1 + 3g_2^2 M_2 + \frac{16}{3}g_3^2 M_3) \\
16\pi^2 \frac{dC''_{ijk}}{dt} &= \lambda''_{lmn}(\lambda''_{imn}C''_{ljk} + 2\lambda''_{ljn}C''_{imk} + 2\lambda''_{lmk}C''_{ijn} \\
&\quad + 4\lambda''_{ijn}C''_{lmk} + 4\lambda''_{imk}C''_{ljn} + 2\lambda''_{ljk}C''_{imn}) \\
&\quad + \lambda'_{lmn}(2\lambda'_{lmj}C''_{ink} + 2\lambda'_{lmk}C''_{ijn} + 4\lambda''_{ijn}C'_{lmk} + 4\lambda''_{ink}C'_{lmj})
\end{aligned} \tag{A.5}$$

$$\begin{aligned}
& +C''_{ijk}(2\delta_{i3}h_t^2 + 2\delta_{j3}h_b^2 + 2\delta_{k3}h_b^2) \\
& +\lambda''_{ijk}(4\delta_{i3}h_t\eta_t + 4\delta_{j3}h_b\eta_b + 4\delta_{k3}h_b\eta_b) \\
& -C''_{ijk}(\frac{4}{3}g_1^2 + 8g_3^2) + \lambda''_{ijk}(\frac{8}{3}g_1^2M_1 + 16g_3^2M_3)
\end{aligned} \tag{A.6}$$

$$\begin{aligned}
16\pi^2 \frac{dm_{e_i e_j}^2}{dt} &= \lambda_{mni}\lambda_{mnk}m_{e_j e_k}^2 + \lambda_{mnj}\lambda_{mnk}m_{e_i e_k}^2 + 4\lambda_{lmi}\lambda_{lnj}m_{L_m L_n}^2 \\
& +m_{e_i e_j}^2(2\delta_{i3}h_\tau^2 + 2\delta_{j3}h_\tau^2) + \delta_{i3}\delta_{j3}(4h_\tau^2m_{H_1}^2 + 4h_\tau^2m_{L_3 L_3}^2 + 4\eta_\tau^2) \\
& +2C_{mni}C_{mnj} + 2\delta_{ij}\xi - 8\delta_{ij}g_1^2M_1^2 \\
16\pi^2 \frac{dm_{L_i L_j}^2}{dt} &= \lambda_{imn}\lambda_{kmn}m_{L_j L_k}^2 + \lambda_{jmn}\lambda_{kmn}m_{L_i L_k}^2 \\
& +3\lambda'_{imn}\lambda'_{kmn}m_{L_j L_k}^2 + 3\lambda'_{jmn}\lambda'_{kmn}m_{L_i L_k}^2 \\
& +2\lambda_{ilm}\lambda_{jln}m_{e_m e_n}^2 + 2\lambda_{iml}\lambda_{jnl}m_{L_m L_n}^2 \\
& +6\lambda'_{ilm}\lambda'_{jln}m_{d_m d_n}^2 + 6\lambda'_{iml}\lambda'_{jnl}m_{Q_m Q_n}^2 \\
& +m_{L_i L_j}^2(\delta_{i3}h_\tau^2 + \delta_{j3}h_\tau^2) + \delta_{i3}\delta_{j3}(2h_\tau^2m_{H_1}^2 + 2h_\tau^2m_{e_3 e_3}^2 + 2\eta_\tau^2) \\
& +2C_{imn}C_{jmn} + 6C'_{imn}C'_{jmn} - \delta_{ij}\xi - 2\delta_{ij}(g_1^2M_1^2 + 3g_2^2M_2^2) \\
16\pi^2 \frac{dm_{Q_i Q_j}^2}{dt} &= \lambda'_{min}\lambda'_{mkn}m_{Q_j Q_k}^2 + \lambda'_{mjn}\lambda'_{mkn}m_{Q_i Q_k}^2 \\
& +2\lambda'_{kim}\lambda'_{kjn}m_{d_m d_n}^2 + 2\lambda'_{mik}\lambda'_{njk}m_{L_m L_n}^2 + 2C'_{min}C'_{mjn} \\
& +m_{Q_i Q_j}^2(\delta_{i3}h_t^2 + \delta_{i3}h_b^2 + \delta_{j3}h_t^2 + \delta_{j3}h_b^2) \\
& +\delta_{i3}\delta_{j3}(2h_t^2m_{H_2}^2 + 2h_t^2m_{u_3 u_3}^2 + 2\eta_t^2 + 2h_b^2m_{H_1}^2 + 2h_b^2m_{d_3 d_3}^2 + 2\eta_b^2) \\
& +\frac{1}{3}\delta_{ij}\xi - 2\delta_{ij}(\frac{1}{9}g_1^2M_1^2 + 3g_2^2M_2^2 + \frac{16}{3}g_3^2M_3^2) \\
16\pi^2 \frac{dm_{u_i u_j}^2}{dt} &= \lambda''_{imn}\lambda''_{kmn}m_{u_j u_k}^2 + \lambda''_{jmn}\lambda''_{kmn}m_{u_i u_k}^2 + 4\lambda''_{ikm}\lambda''_{jkn}m_{d_m d_n}^2 + 2C''_{imn}C''_{jmn} \\
& +m_{u_i u_j}^2(2\delta_{i3}h_t^2 + 2\delta_{j3}h_t^2) + \delta_{i3}\delta_{j3}(4h_t^2m_{H_2}^2 + 4h_t^2m_{Q_3 Q_3}^2 + 4\eta_t^2) \\
& -\frac{4}{3}\delta_{ij}\xi - 2\delta_{ij}(\frac{16}{9}g_1^2M_1^2 + \frac{16}{3}g_3^2M_3^2) \\
16\pi^2 \frac{dm_{d_i d_j}^2}{dt} &= 2\lambda'_{mni}\lambda'_{mnk}m_{d_j d_k}^2 + 2\lambda'_{mnj}\lambda'_{mnk}m_{d_i d_k}^2 \\
& +2\lambda''_{mni}\lambda''_{mnk}m_{d_j d_k}^2 + 2\lambda''_{mnj}\lambda''_{mnk}m_{d_i d_k}^2 \\
& +4\lambda'_{kmi}\lambda'_{knj}m_{Q_m Q_n}^2 + 4\lambda'_{mki}\lambda'_{nkj}m_{L_m L_n}^2 \\
& +4\lambda''_{kmi}\lambda''_{knj}m_{d_m d_n}^2 + 4\lambda''_{mki}\lambda''_{nkj}m_{u_m u_n}^2 \\
& +4C'_{mni}C'_{mnj} + 4C''_{mni}C''_{mnj} \\
& +m_{d_i d_j}^2(2\delta_{i3}h_b^2 + 2\delta_{j3}h_b^2) + \delta_{i3}\delta_{j3}(4h_b^2m_{H_1}^2 + 4h_b^2m_{Q_3 Q_3}^2 + 4\eta_b^2)
\end{aligned}$$

$$+\frac{2}{3}\delta_{ij}\xi - 2\delta_{ij}(\frac{4}{9}g_1^2M_1^2 + \frac{16}{3}g_3^2M_3^2) \quad (\text{A.7})$$

In the above equations, we have not allowed for the inclusion of Yukawa terms other than those of the third generation, and we have also not presented dimensionful terms such as $m_{L_i H_1}^2$ which can be generated by the mixing of L_i and H_1 . However, these may be trivially derived from the above by simply regarding H_1 as L_4 , dropping the explicit h_b and h_τ dependence of the equations, and setting

$$\lambda_{343} = -\lambda_{433} = h_\tau \quad \lambda'_{433} = -h_b \quad C_{343} = -C_{433} = \eta_\tau \quad C'_{433} = -\eta_b \quad (\text{A.8})$$

Adopting this notation, we find

$$\begin{aligned} 16\pi^2 \frac{d\mu_i}{dt} &= \mu_i(3h_t^2 - g_1^2 - 3g_2^2) + 3\lambda'_{ikl}\lambda'_{jkl}\mu_j + \lambda_{ikl}\lambda_{jkl}\mu_j \\ 16\pi^2 \frac{dD_i}{dt} &= D_i(3h_t^2 - g_1^2 - 3g_2^2) + 3\lambda'_{ikl}\lambda'_{jkl}D_j + \lambda_{ikl}\lambda_{jkl}D_j \\ &\quad + 6h_t\eta_t\mu_i + 6C'_{ikl}\lambda'_{jkl}\mu_j + 2C_{ikl}\lambda_{jkl}\mu_j + 2g_1^2M_1\mu_i + 6g_2^2M_2\mu_i \end{aligned} \quad (\text{A.9})$$

We further note that although we have given the RGEs for the third generation Yukawas only, it is straightforward to use this notation to generate the full RGEs including general mass matrices and the full CKM dependence through

$$\lambda'_{4ij} = -h_{ij}^d \quad (\text{A.10})$$

where h_{ij}^d is the full Yukawa matrix for the down-type quarks, which can at low energies be found from the quark masses and the CKM matrix as defined, for example, in [22]. In general, the R-parity violating couplings will prevent all the mass matrices remaining diagonal even if they are initially so chosen, as discussed above.

For completeness, we also give the RGE for $m_{H_2 H_2}^2$, which is unchanged from that of the MSSM.

$$\begin{aligned} 16\pi^2 \frac{dm_{H_2 H_2}^2}{dt} &= 6h_t^2(m_{Q_3 Q_3}^2 + m_{H_2 H_2}^2 + m_{u_3 u_3}^2) + 6\eta_t^2 \\ &\quad - (2g_1^2M_1^2 + 6g_2^2M_2^2) + \xi \end{aligned} \quad (\text{A.11})$$

B Definition of Functions

The expressions for the amplitudes in $\mu \rightarrow e\gamma$ presented earlier employ a number of functions, most of which can be found in either ref. [27] or in Appendix B of ref. [28].

We repeat the definitions here for convenience.

$$\begin{aligned}
F_1(x) &= \frac{1}{12(x-1)^4} [x^3 - 6x^2 + 3x + 2 + 6x \ln(x)] \\
F_2(x) &= \frac{1}{x} F_1\left(\frac{1}{x}\right) \\
&= \frac{1}{12(x-1)^4} [2x^3 + 3x^2 - 6x + 1 - 6x^2 \ln(x)] \\
F_3(x) &= \frac{1}{2(x-1)^3} [x^2 - 4x + 3 + 2 \ln(x)] \\
F_4(x) &= \frac{1}{2(x-1)^3} [x^2 - 1 - 2x \ln(x)] \\
G(x) &= F_1(x) + xF_1'(x) \\
&= \frac{1}{6(x-1)^5} [x^3 + 9x^2 - 9x - 1 - 6x(x+1) \ln(x)] \\
F(x) &= F_2(x) + xF_2'(x) \\
&= \frac{1}{12(x-1)^5} [-17x^3 + 9x^2 + 9x - 1 + 6x^2(x+3) \ln(x)] \\
H(x) &= F_3(x) + xF_3'(x) \\
&= \frac{1}{2(x-1)^4} [x^2 + 4x - 5 - 2(2x+1) \ln(x)] \\
L(x) &= F_4(x) + xF_4'(x) \\
&= \frac{1}{2(x-1)^4} [-5x^2 + 4x + 1 + 2x(x+2) \ln(x)] \tag{B.1}
\end{aligned}$$

Here the prime simply indicates the first derivative. Certain asymptotic values of these functions are useful, as listed in Table 2 below.

x	$F_1(x)$	$F_2(x)$	$F_3(x)$	$F_4(x)$	$G(x)$	$F(x)$	$H(x)$	$L(x)$
0	1/6	1/12	$-\ln(x)$	1/2	1/6	1/12	$-\ln(x) - 5/2$	1/2
1	1/24	1/24	1/3	1/6	1/60	1/40	1/12	1/12
∞	1/12x	1/6x	1/2x	1/2x	1/6x ²	$\ln(x)/2x^2$	1/2x ²	$\ln(x)/x^2$

Table 2. Values of the various functions in useful limits.

References

- [1] For reviews see for example H.P. Nilles, *Phys. Rep.* **110** (1984) 1;
H.E. Haber and G.L. Kane, *Phys. Rep.* **117** (1985) 75.
- [2] C.S. Aulakh, R.N. Mohapatra, *Phys. Lett.* **B119** (1982) 316;
F. Zwirner, *Phys. Lett.* **B132** (1983) 103;
S. Dawson, *Nucl. Phys.* **B261** (1985) 297;
R. Barbieri, A. Masiero, *Nucl. Phys.* **B267** (1986) 679;
S. Dimopoulos, L.J. Hall, *Phys. Lett.* **B196** (1987) 135.
- [3] L.J. Hall, M. Suzuki, *Nucl. Phys.* **B231** (1984) 419.
- [4] H. Dreiner, G.G. Ross, *Nucl. Phys.* **B410** (1993) 188.
- [5] B. Brahmachari, P. Roy, *Phys.Rev.* **D50** (1994) R39; and errata in *Phys.Rev.* **D51** (1995) 3974.
- [6] J.L. Goity, M. Sher, *Phys. Lett.* **B346** (1995) 69.
- [7] H. Dreiner, H. Pois, hep-ph/9511444.
- [8] V. Barger, M.S. Berger, R.J.N. Phillips, T. Wohrmann, hep-ph/9511473.
- [9] V. Barger, G.F. Giudice, T. Han, *Phys. Rev.* **D40** (1989) 2987.
- [10] V. Barger, R.J.N. Phillips, K. Whisnant, *Phys. Rev.* **D44** (1991) 1629.
- [11] T. Banks, Y. Grossman, E. Nardi, Y. Nir, *Phys. Rev.* **D52** (1995) 5319.
- [12] L.E. Ibáñez, C. López, *Nucl. Phys.* **B233** (1984) 511.
- [13] K. Agashe, M. Graesser, hep-ph/9510439.
- [14] J. Hagelin, S. Kelley, T. Tanaka, *Nucl. Phys.* **B415** (1994) 293;
J. Hagelin, S. Kelley, T. Tanaka, *Mod. Phys. Lett.* **A8** (1993) 2737

- [15] L.J. Hall, V.A. Kostelecky, S. Raby, *Nucl. Phys.* **B267** (1986) 415;
F. Gabbiani, A. Masiero, *Nucl. Phys.* **B322** (1989) 235;
G.C. Branco, G.C. Cho, Y. Kizukuri, N. Oshimo, *Phys. Lett.* **B337** (1994) 316;
R. Barbieri, L. Hall, A. Strumia, *Nucl. Phys.* **B445** (1995) 219; *Nucl. Phys.*
B449 (1995) 437
- [16] I. Lee, *Nucl. Phys.* **B246** (1984) 120.
- [17] J.C. Romao, J.W.F. Valle, *Nucl. Phys.* **B381** (1992) 87.
- [18] A. Smirnov, F. Vissani, *Nucl. Phys.* **B460** (1996) 37.
- [19] R. Barbieri, M.M. Guzzo, A. Masiero, D. Tommasini, *Phys. Lett.* **B252** (1990) 251.
- [20] K. Enqvist, A. Masiero, A. Riotto, *Nucl. Phys.* **B373** (1992) 95.
- [21] R. Hempfling, hep-ph/9511288.
- [22] Particle Data Group Review of Particle Properties, *Phys. Rev.* **D50** (1994) 1173.
- [23] K.S. Babu, R.N. Mohapatra, *Phys. Rev. Lett.* **75** (1995) 2276.
- [24] J.-P. Derendinger, C.A. Savoy, *Nucl. Phys.* **B237** (1984) 307.
- [25] R.D. Bolton et al., *Phys. Rev.* **D38** (1988) 2077.
- [26] D. Choudhury, F. Eberlein, A. König, J. Louis and S. Pokorski, *Phys. Lett.* **B342** (1995) 180;
S. Dimopoulos and D. Sutter, *Nucl. Phys.* **B452** (1995) 496;
E. Gabrielli, A. Masiero and L. Silvestrini, hep-ph/9509379.
- [27] B. de Carlos, J.A. Casas and J.M. Moreno, *Phys. Rev.* **D53** (1996) 6398.
- [28] S. Bertolini, F. Borzumati, A. Masiero, G. Ridolfi, *Nucl. Phys.* **B353** (1991) 591.

- [29] J.F. Gunion and H.E. Haber, *Nucl. Phys.* **B272** (1986) 1, and errata in *Nucl. Phys.* **B402** (1993) 567.
- [30] S.P. Martin, M.T. Vaughn, *Phys. Rev.* **D50** (1994) 2282.

C Figure Captions

Figure 1: Feynman diagrams contributing to $L_i - H_1$ mixing and hence to the generation of sneutrino VEVs. We do not show possible mass insertions on the lines.

Figure 2a: Absolute values of the sneutrino VEV (dashed lines) and corresponding neutrino mass (solid lines) as a function of m_{L_i} , with parameters $m_t = 175\text{GeV}$, $\alpha_3(M_Z) = 0.12$, $\tan\beta = 2$ and 20 , $M_{1/2} = 500\text{GeV}$, $A_0 = 0$, both signs of μ , and $\lambda_{133}(M_{GUT}) = 0.01$.

Figure 2b: Absolute values of the sneutrino VEV (dashed lines) and corresponding neutrino mass (solid lines) as a function of m_{L_i} , with parameters $m_t = 175\text{GeV}$, $\alpha_3(M_Z) = 0.12$, $\tan\beta = 2$ and 20 , $M_{1/2} = 500\text{GeV}$, $A_0 = 0$, both signs of μ , and $\lambda'_{133}(M_{GUT}) = 0.001$.

Figure 3: Absolute values of the sneutrino VEV (dashed lines) and corresponding neutrino mass (solid lines) as a function of $M_{1/2}$, with parameters $m_t = 175\text{GeV}$, $\alpha_3(M_Z) = 0.12$, $\tan\beta = 2$, 20 , $m_{L_i} = 500\text{GeV}$, $A_0 = 0$, both signs of μ , and $\lambda'_{133}(M_{GUT}) = 0.001$.

Figure 4: Absolute values of the sneutrino VEV (dashed lines) and corresponding neutrino mass (solid lines) as a function of A_0 , with parameters $m_t = 175\text{GeV}$, $\alpha_3(M_Z) = 0.12$, $\tan\beta = 2$ and 20 , $M_{1/2} = m_{L_i} = 500\text{GeV}$, both signs of μ , and $\lambda'_{133}(M_{GUT}) = 0.001$.

Figures 5: Diagrams contributing to \tilde{A}_{LR}^λ . The analogous contributions to \tilde{A}_{RL}^λ have a left handed internal lepton line. All diagrams are presented without photon lines for clarity, and the crosses indicate helicity flips except where otherwise marked.

Figure 6: Diagrams contributing to $\tilde{A}_{LR}^{\lambda'}$. There are no analogous diagrams for $\tilde{A}_{RL}^{\lambda'}$.

Figure 7: Diagrams contributing to $\tilde{A}_{LR}^{\Delta m}$. The analogous contribution to $\tilde{A}_{RL}^{\Delta m}$ is proportional to the electron mass in the chargino case and hence neglected, while for

the RL neutralino case right and left handed fields are interchanged.

Figures 8: Examples of diagrams which contribute to \tilde{A}_{LR}^λ with the insertion of a sneutrino VEV and hence neutralino-neutrino or slepton-chargino mixing.

Figure 9: Absolute values of amplitudes for $\mu \rightarrow e\gamma$ from direct R-parity violation diagrams (dashed lines), neutralino mediated diagrams (dot-dashed lines), and chargino mediated diagrams (dotted lines) plotted against $M_{1/2}$. We also show the total amplitude (solid line) and the experimental bound on the amplitude (horizontal solid line). Parameters are $m_t = 175\text{GeV}$, $\alpha_3(M_Z) = 0.12$, $\tan\beta = 10$, $m_0 = 100\text{GeV}$, $A_0 = 0$, $\mu_4 > 0$, and $\lambda'_{111}(M_{GUT}) = \lambda'_{211}(M_{GUT}) = 0.001$.

Figure 10: Exactly as for Figure 9, but varying m_0 and with $M_{1/2}$ set to 100GeV .

Figure 11: Exactly as for Figure 9, but varying A_0 with both m_0 and $M_{1/2}$ set to 100GeV .

Figure 12: Exactly as for Figure 9, but with $\tan\beta = 30$.

Figure 13: Absolute values of amplitudes for $\mu \rightarrow e\gamma$ from direct R-parity violation diagrams (dashed lines), neutralino mediated diagrams (dot-dashed lines), and chargino mediated diagrams (dotted lines) plotted against $M_{1/2}$. We also show the total amplitude (solid line) and the experimental bound on the amplitude (horizontal solid line). Parameters are $m_t = 175\text{GeV}$, $\alpha_3(M_Z) = 0.12$, $\tan\beta = 10$, $m_0 = 100\text{GeV}$, $A_0 = 0$, $\mu_4 > 0$, and $\lambda_{131}(M_{GUT}) = \lambda_{231}(M_{GUT}) = 0.01$.

Figure 14: Similar to Figure 13, but varying A_0 . Parameters are $m_t = 175\text{GeV}$, $\alpha_3(M_Z) = 0.12$, $\tan\beta = 2$, $M_{1/2} = m_0 = 100\text{GeV}$, $A_0 = 0$, $\mu_4 > 0$, and $\lambda_{131}(M_{GUT}) = \lambda_{231}(M_{GUT}) = 0.01$.

Figure 15: Absolute values of amplitudes for $\mu \rightarrow e\gamma$ from direct R-parity violation diagrams (dashed lines), and neutralino mediated diagrams (dot-dashed lines) plotted against $M_{1/2}$. We also show the total amplitude (solid line) and the experimen-

tal bound on the amplitude (horizontal solid line). Parameters are $m_t = 175\text{GeV}$, $\alpha_3(M_Z) = 0.12$, $\tan\beta = 10$, $m_0 = 100\text{GeV}$, $A_0 = 0$, $\mu_4 > 0$, and $\lambda_{121}(M_{GUT}) = \lambda_{122}(M_{GUT}) = 0.01$.

Figure 1a

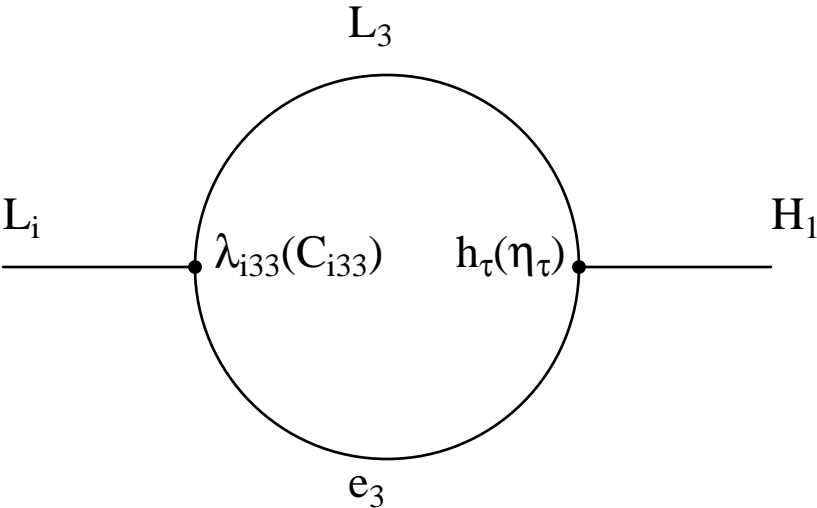


Figure 1b

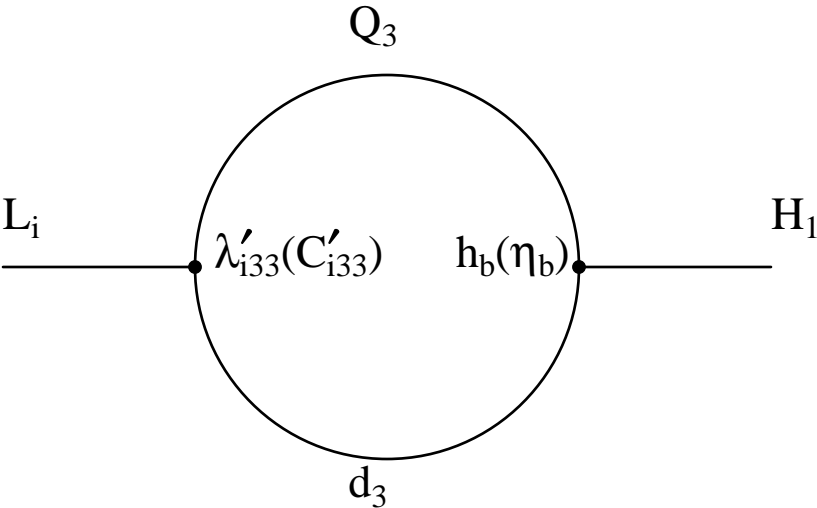


Figure 2a

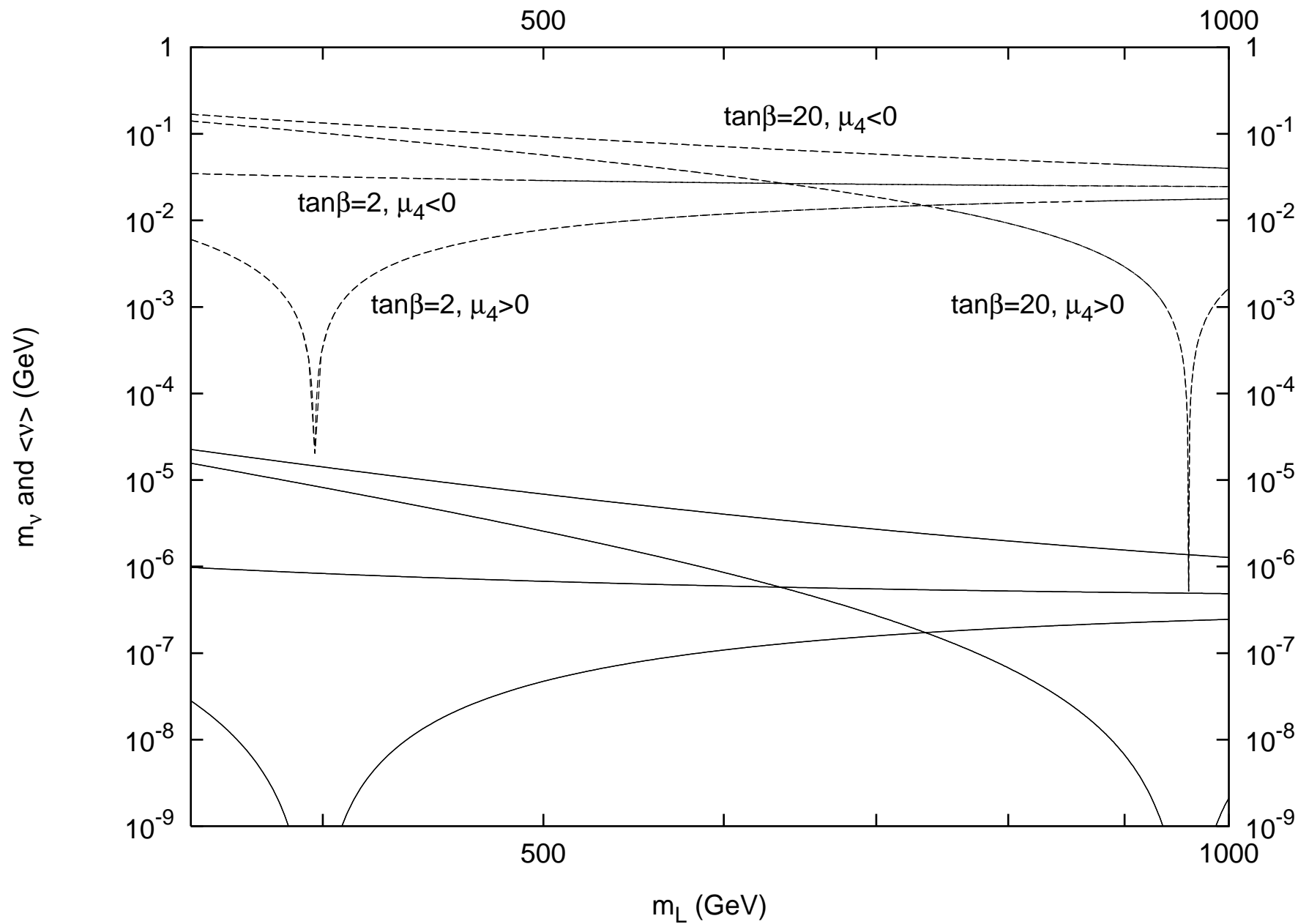


Figure 2b

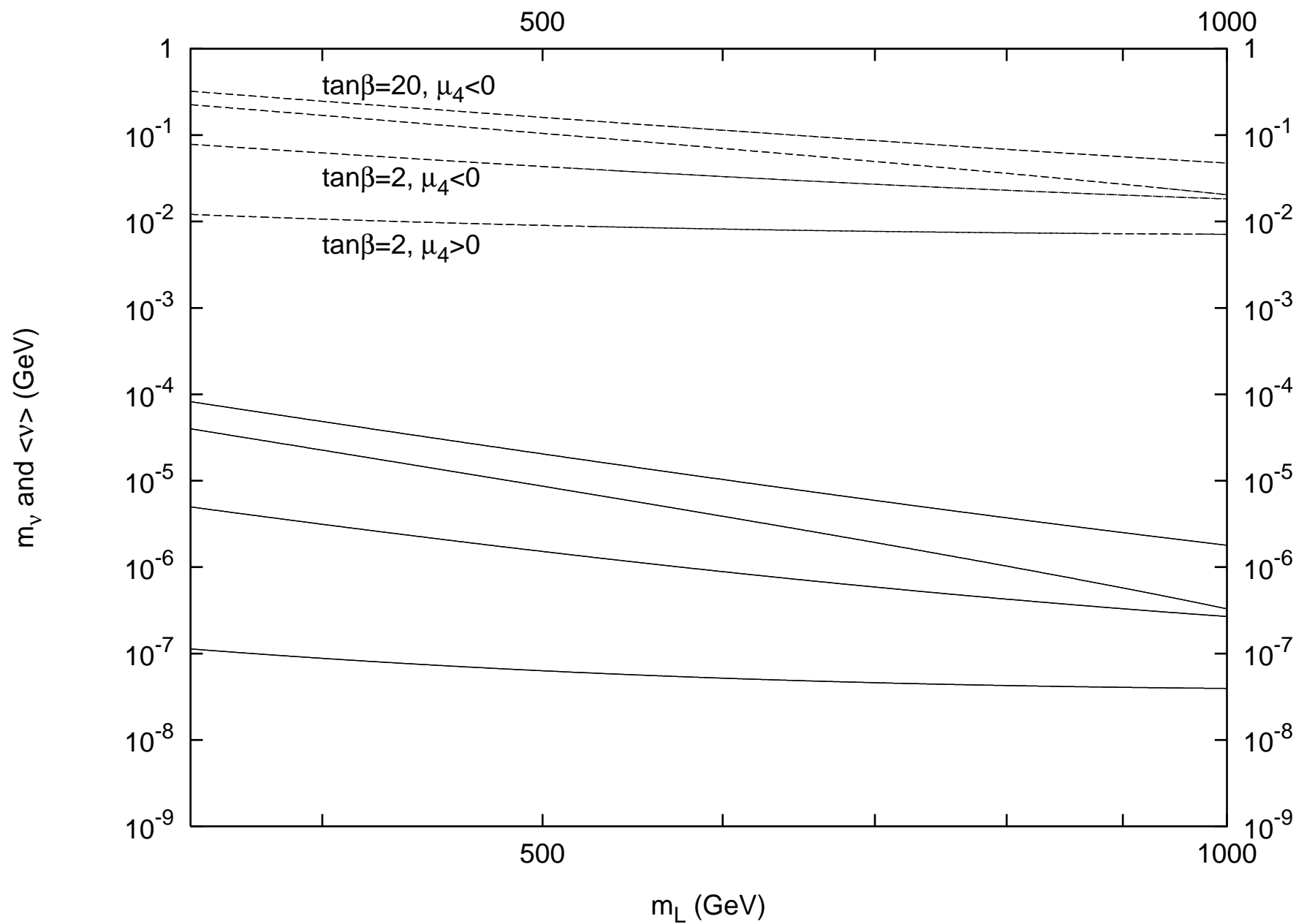


Figure 3

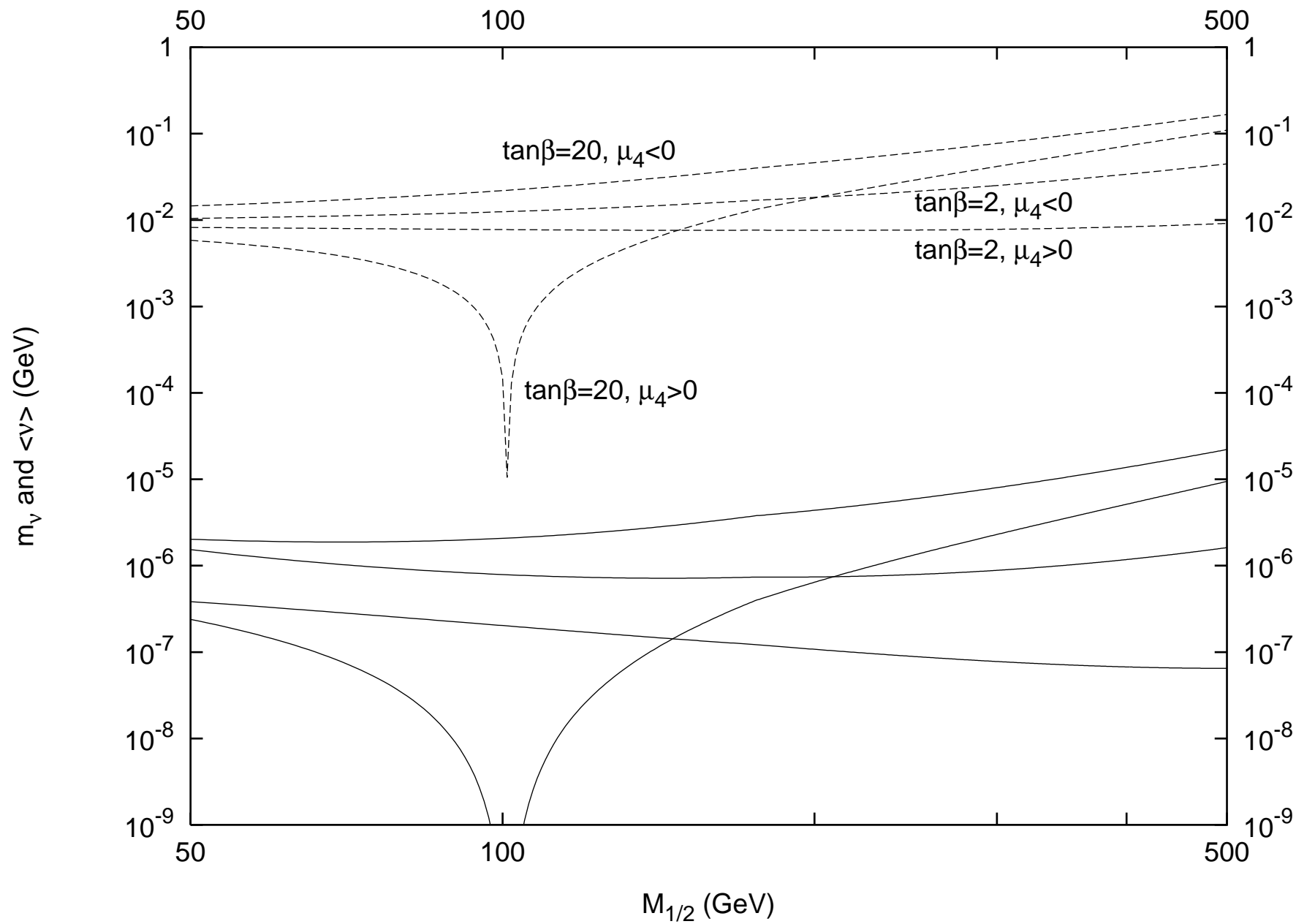


Figure 4

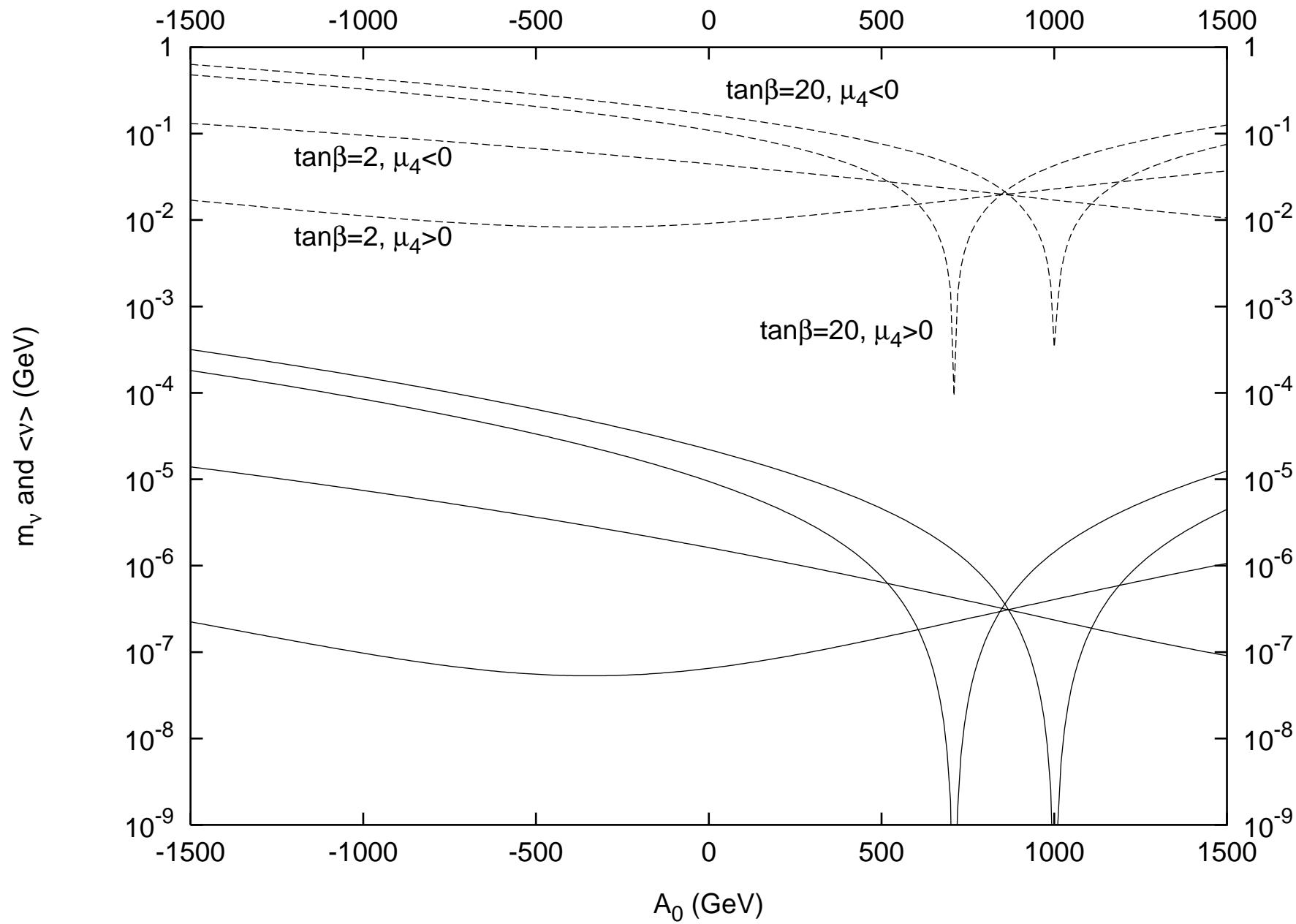


Figure 7a

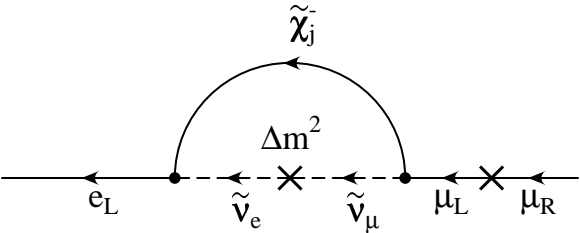


Figure 7b

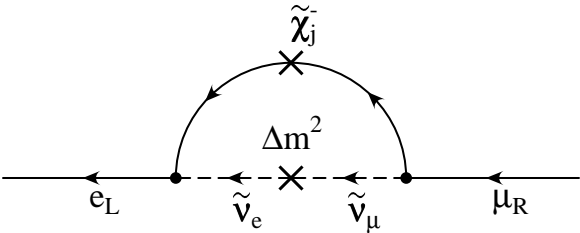


Figure 7c

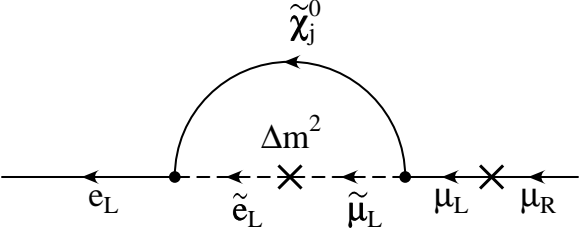


Figure 7d

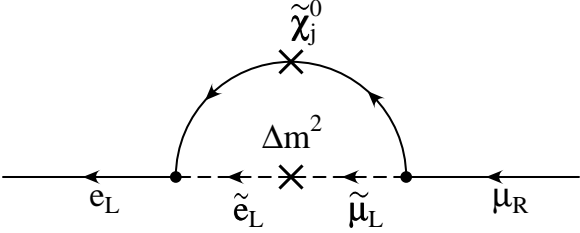


Figure 7e

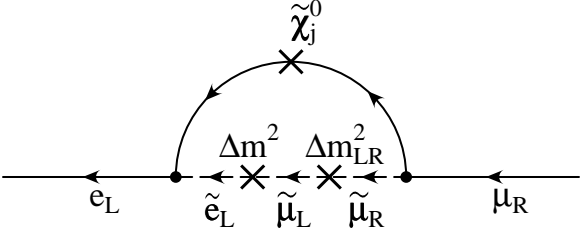


Figure 8a

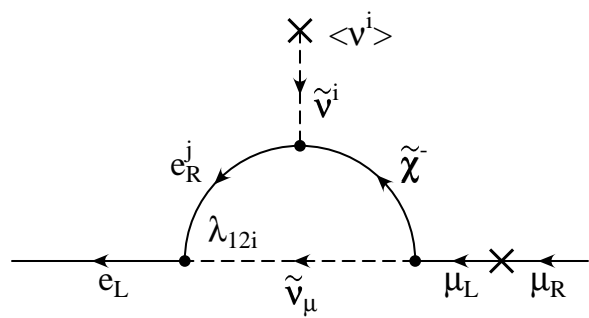


Figure 8b

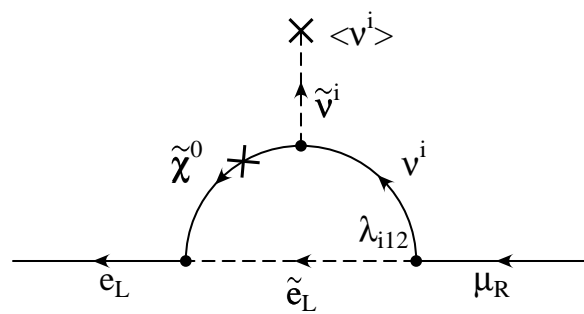


Figure 9

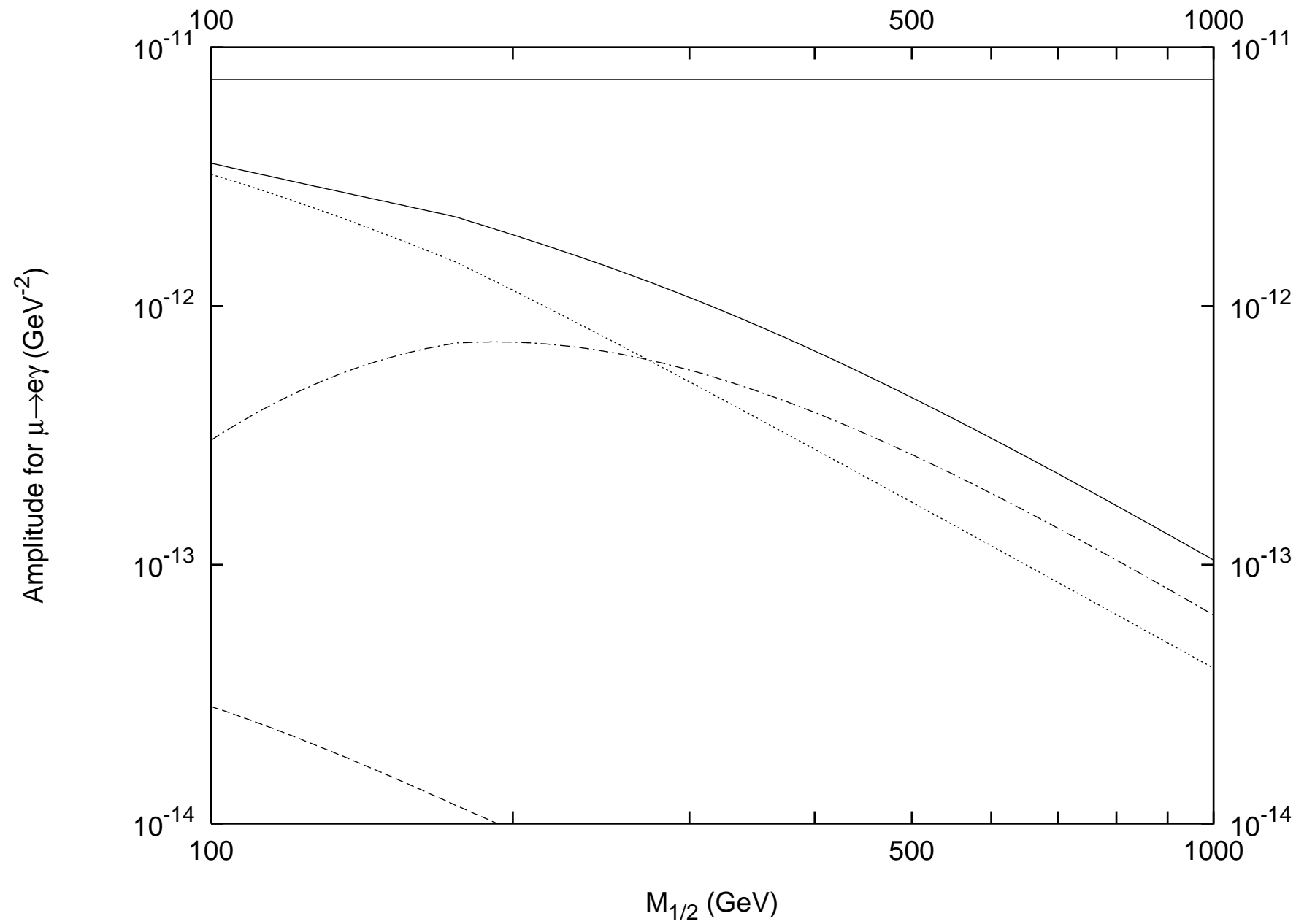


Figure 10

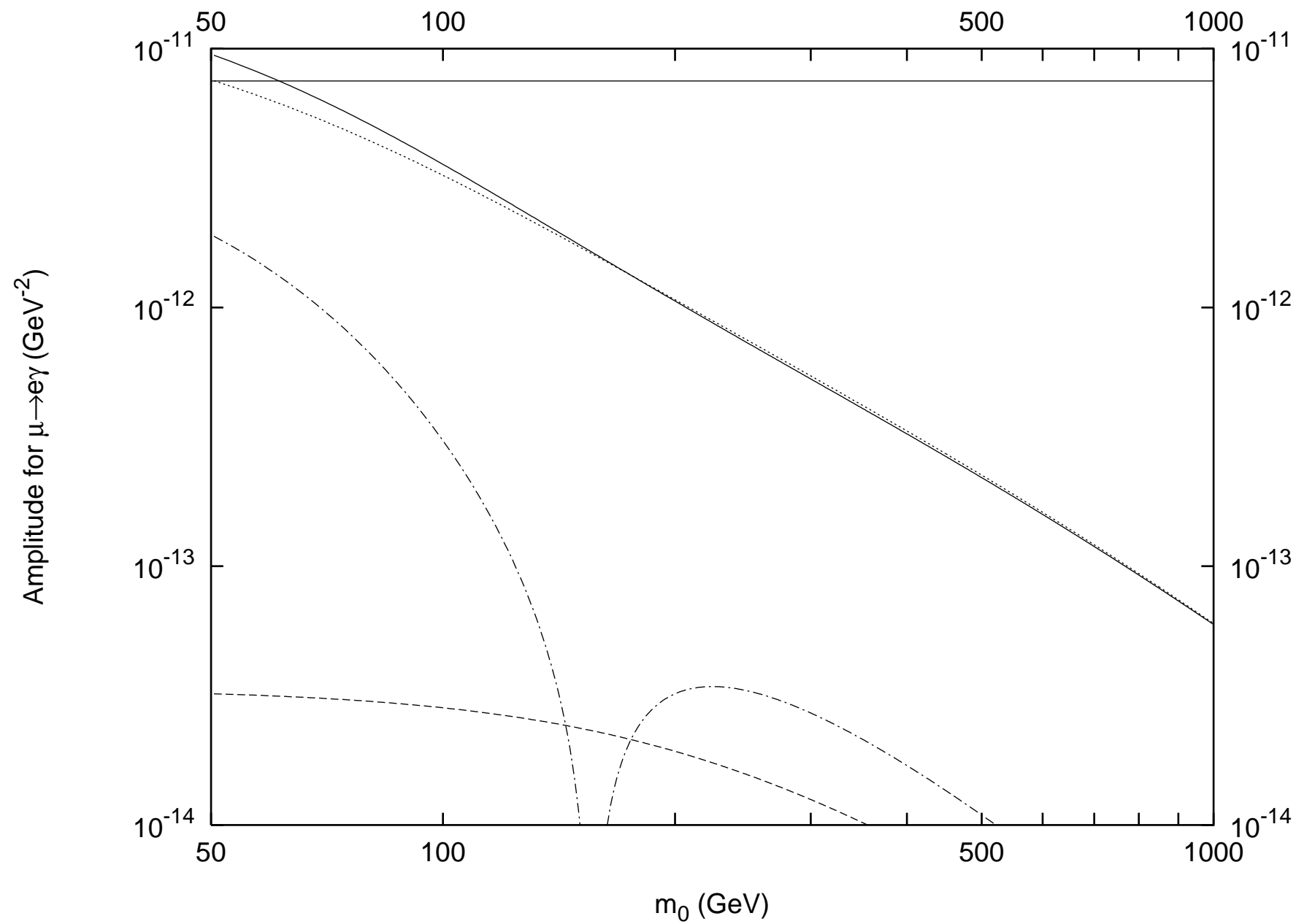


Figure 11

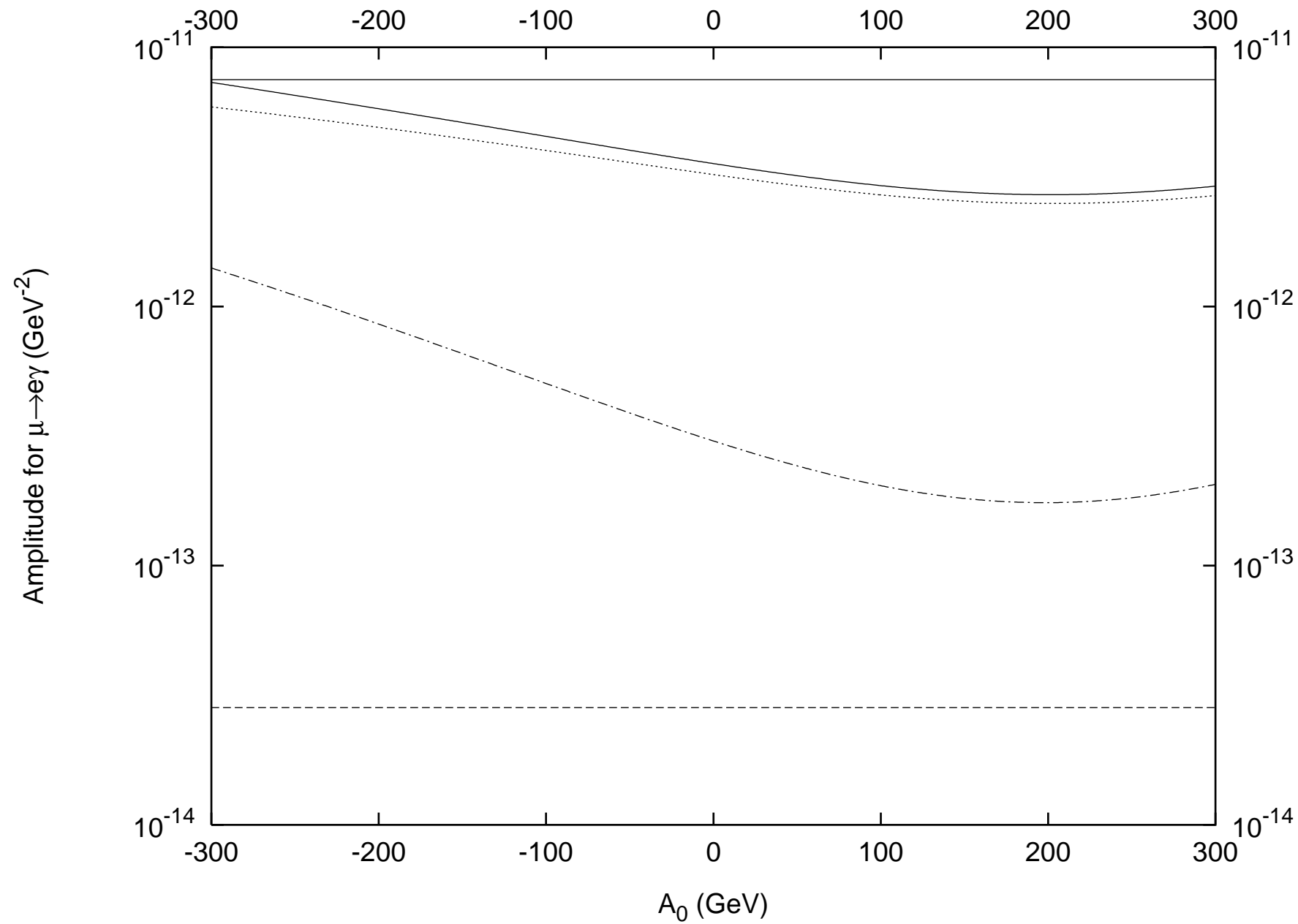


Figure 12

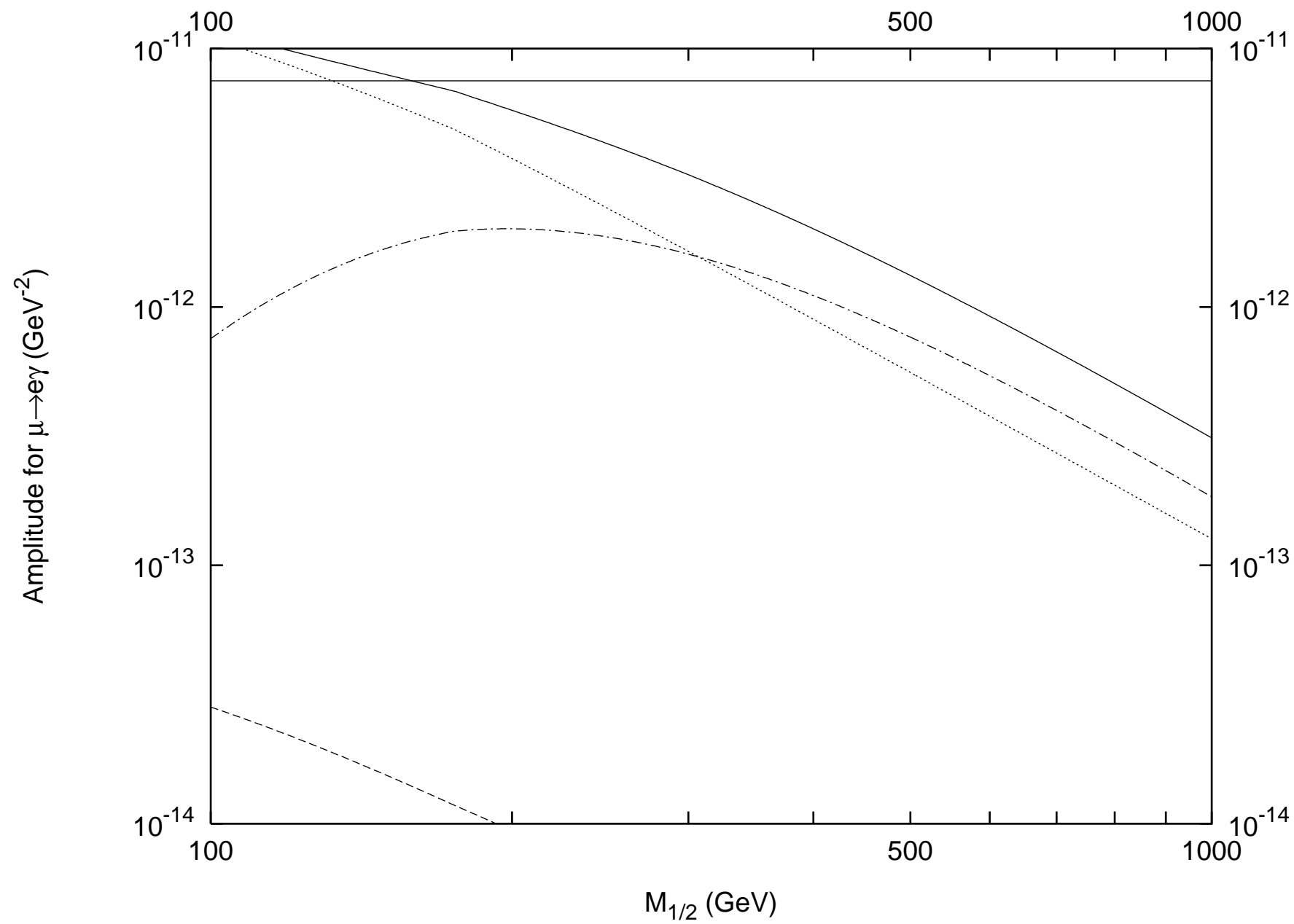


Figure 13

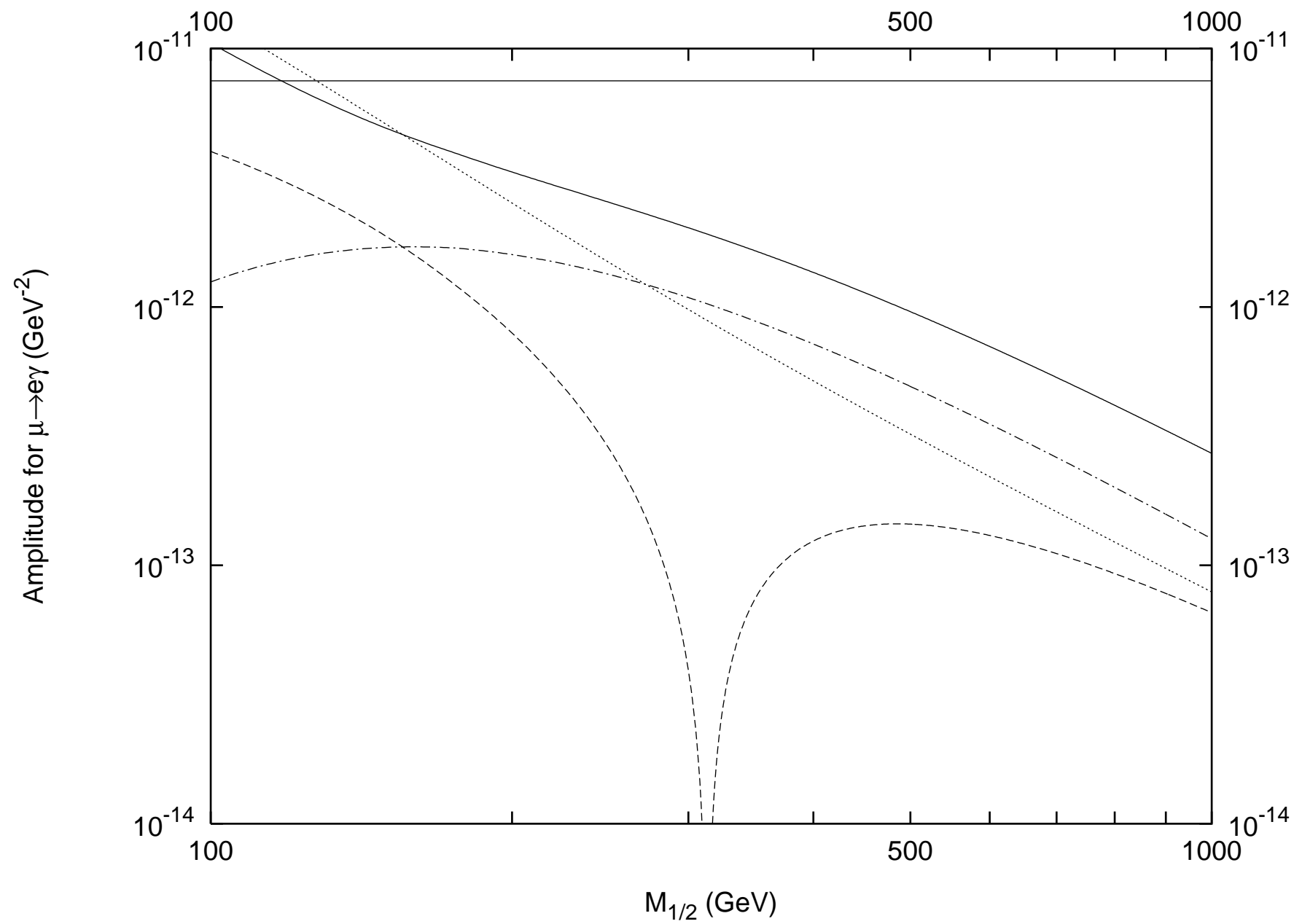


Figure 14

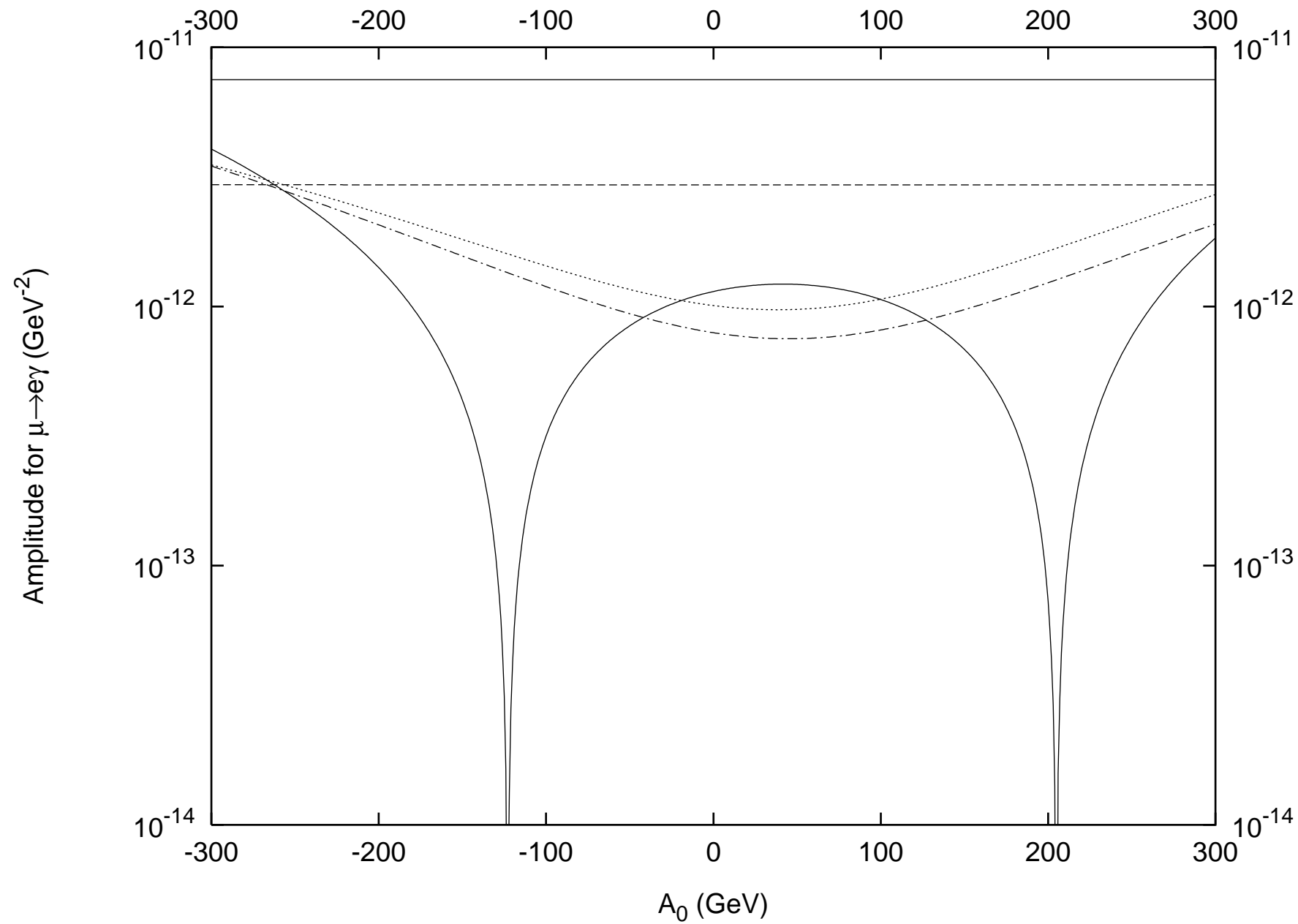


Figure 15

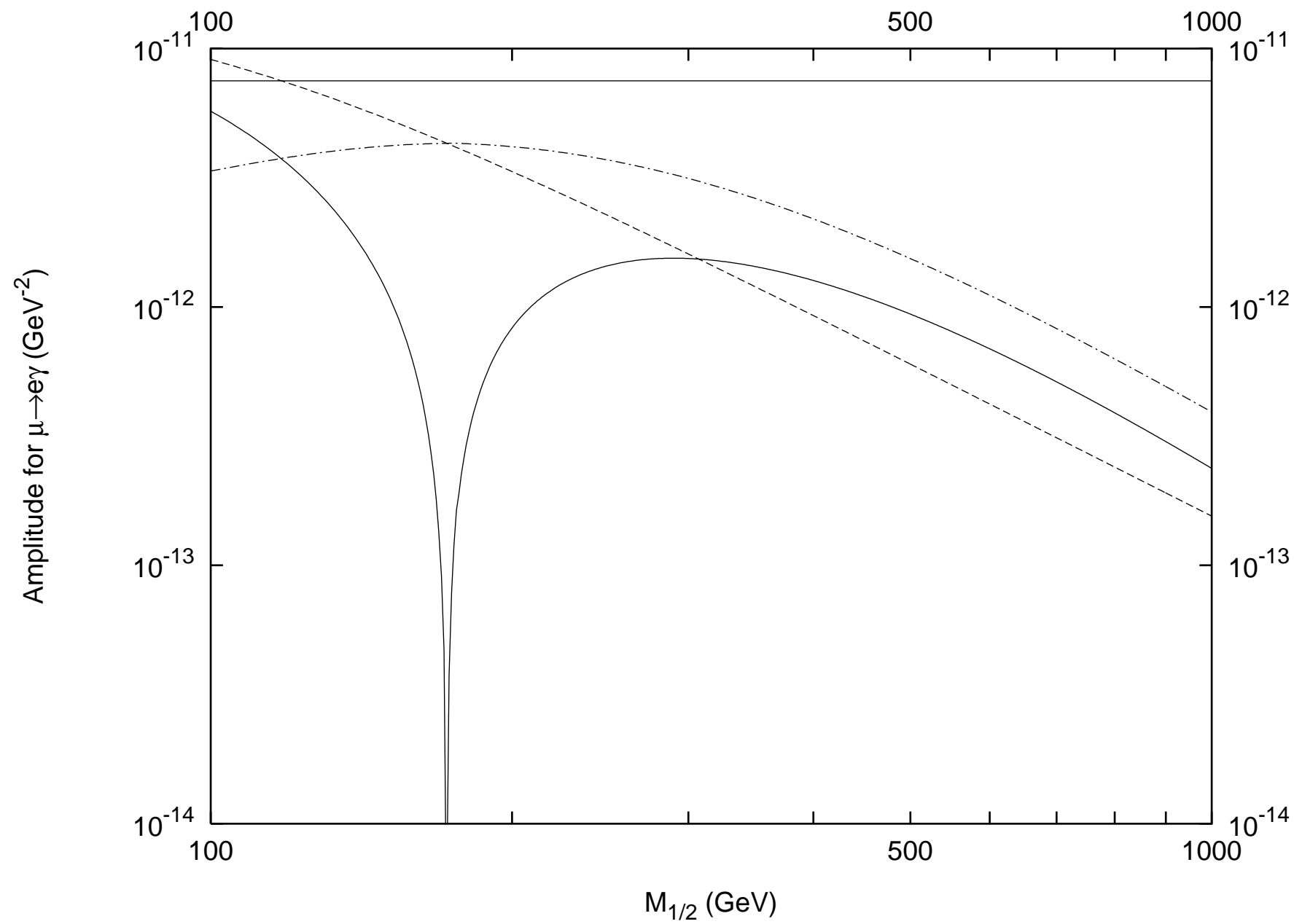


Figure 5a

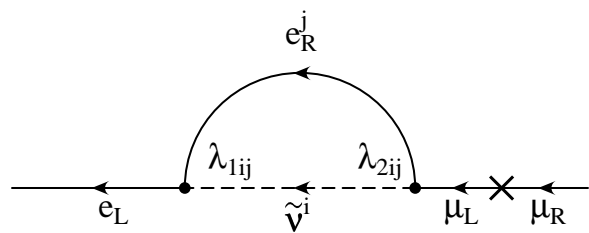


Figure 5b

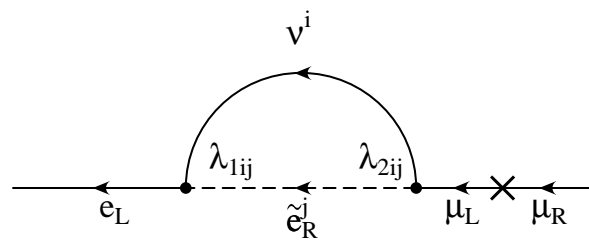


Figure 6a

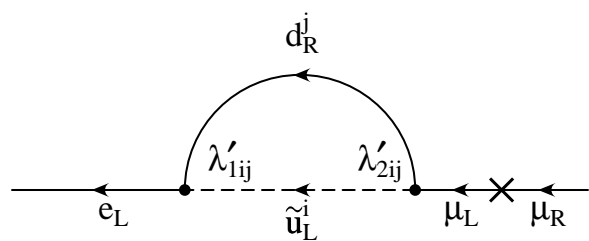


Figure 6b

